# From urine to food and oxygen: effects of high and low $NH_4^+$:$NO_3^-$ ratio on lettuce cultivated in a gas-tight hydroponic facility

Mona Schiefloe[1*†], Øyvind Mejdell Jakobsen[1*†],
Antonio Pannico[2], Claudia Quadri[3] and Ann-Iren Kittang Jost[1]

[1]Centre for Interdisciplinary Research in Space (CIRiS), NTNU Social Research, Trondheim, Norway,
[2]Department of Agricultural Sciences, University of Naples Federico II, Portici, Italy, [3]EnginSoft Società
per Azioni, Bergamo, Italy

*In situ* production of food, water and oxygen is essential for long-duration human space missions. Higher plants represent a key element in Bioregenerative Life Support Systems (BLSS), where crop cultivation can be based on water and nutrients recovered from waste and wastewater. Human urine exemplifies an important waste stream with potential to provide crops with nitrogen (N) and other nutrients. Dynamic waste composition and treatment processes may result in mineralized fractions with varying ammonium ($NH_4^+$) to nitrate ($NO_3^-$) ratios. In this study, lettuce was cultivated in the unique ESA MELiSSA Plant Characterization Unit, an advanced, gas-tight hydroponic research facility offering controlled environment and continuous monitoring of atmospheric gas composition. To evaluate biological and system effects of nutrient solution $NH_4^+$:$NO_3^-$ ratio, two crop tests were run with different $NH_4^+$ to total N ratio ($NH_4^+$:N) and elevated concentrations of $Na^+$ and $Cl^-$ in line with a urine recycling scenario. Plants cultivated at 0.5 mol·mol$^{-1}$ $NH_4^+$:N ($HiNH_4^+$) achieved 50% lower shoot biomass compared to those cultivated at 0.1 mol·mol$^{-1}$ $NH_4^+$:N ($LoNH_4^+$), accompanied by higher shoot dry weight content and lower harvest index. Analyses of projected leaf area over time indicated that the reduced biomass observed at harvest could be attributed to a lower specific growth rate during the close-to-exponential growth phase. The $HiNH_4^+$ crop produced 40% less $O_2$ over the full cultivation period. However, normalization of the results indicated a marginal increase in $O_2$ production per time and per projected leaf area for the $HiNH_4^+$ crop during the exponential growth phase, in line with a higher shoot chlorophyll content. Mineral analysis demonstrated that the biomass content of $NH_4^+$ and $NO_3^-$ varied in line with the nutrient solution composition. The ratio of consumed $NH_4^+$ to consumed N was higher than the $NH_4^+$:N ratio of the nutrient solution for both crop tests, resulting in decreasing $NH_4^+$:N ratios in the nutrient solution over time. The results provide enhanced insight for design of waste processes and crop cultivation to optimize overall BLSS efficiency and hold valuable potential for improved resource utilization also in terrestrial food production systems.

# 1 Introduction

Human spaceflight missions to remote locations call for on-site food production and resource recirculation. In contrast to Low Earth Orbit, complete resupply of resources from Earth is challenged by increased mission duration and travel distances. Higher plants represent a key element for regeneration of air, water and food for astronauts (Wheeler et al., 2002; Pannico et al., 2022), either as part of stand-alone Bioregenerative Life Support Systems (BLSS), or in a combination with physicochemical methods. The MELiSSA project (Micro Ecological Life Support System Alternative) is an international collaboration led by the European Space Agency (ESA), emphasizing the development of a BLSS to support long-term space missions. In an integrated loop, waste streams from a crew compartment are to be processed by thermophilic, heterotrophic and nitrifying bacteria to provide input to photosynthetic compartments with higher plants and algae to regenerate mineralized nutrients and carbon dioxide ($CO_2$), and produce food, pure water, and oxygen ($O_2$) for the crew (Godia et al., 2002). An important objective of the MELiSSA project is to develop mathematical models that can predict critical processes such as plant growth, photosynthesis, and transpiration, based on parameters such as plant species, cultivation conditions, and the processed waste stream fed to the plants.

In a scenario of crop cultivation based on mineralized human waste, urine is a valuable resource due to its high nitrogen (N) content. N is an essential element and a critical input factor for crop cultivation, with profound effects on plant growth and development as a constituent of numerous vital compounds such as nucleic acids, chlorophyll, amino acids, proteins, ATP, phytohormones, auxin and cytokinins (Marschner and Marschner, 2012; Taiz, 2015; De Bang et al., 2021). The use of recycled organic waste for crop cultivation typically requires mineralization of organic compounds by physicochemical and/or microbial processes. N is primarily taken up by plant roots as inorganic ammonium ($NH_4^+$) and nitrate ($NO_3^-$) (Marschner and Marschner, 2012; Taiz, 2015), that may be derived from urine. While fresh urine is rich in urea-N (up to 12 g $L^{-1}$), this compound is rapidly hydrolyzed upon storage in a non-sterile environment to $NH_4^+/NH_3$ that may be further converted to $NO_3^-$ by physicochemical and/or microbial processes (Udert et al., 2006; Larsen et al., 2021). As the result of this upstream treatment depends on the mineralization strategy and the process conditions, the resulting nutrient solution provided to the plants may vary in the absolute concentrations of $NH_4^+$ and $NO_3^-$ and the ratio between them. This may in turn affect not only the plant uptake rates of these inorganic N species, but also other physiological and metabolic processes such as uptake of other nutrients, enzyme activity, photosynthesis and respiration, water balance, signaling pathways, leaf expansion, and root architecture - eventually influencing the overall plant growth and crop yield (Guo et al., 2007a; Guo et al., 2007c; Andrews et al., 2013; Liu and Von Wiren, 2017). A nutrient solution containing both $NH_4^+$ and $NO_3^-$ is typically preferred to optimize plant growth and development rather than using either $NO_3^-$ or $NH_4^+$ as the sole source of N,

although the use of $NH_4^+$ as the dominant N source should be avoided to reduce risk of ammonium toxicity and reduced plant growth (Roosta and Schjoerring, 2008; Taiz, 2015; Song et al., 2021; Weil et al., 2021; Hameed et al., 2022). Beyond N, urine contains other plant macronutrients such as potassium, phosphorus, sulfur, and lower levels of calcium and magnesium (Udert et al., 2006; Larsen et al., 2021). On the other hand, feeding crops with processed urine introduces non-essential elements such as sodium ($Na^+$) and chloride ($Cl^-$). Plants naturally accumulate salts, and the presence of $Na^+$ and $Cl^-$ in the nutrient solution may affect plant physiology and growth. At some concentrations, NaCl has been demonstrated to act as a eustressor with beneficial effects on crop quality (Kronzucker et al., 2013; Rouphael et al., 2018). However, high concentrations of salt is among the most limiting factors for plant growth and may cause injurious abiotic stress, altering morphological and physiological plant traits and ultimately reducing crop yield (Chinnusamy and Zhu, 2006; Acosta-Motos et al., 2017).

To make possible a new generation of scientific studies related to the higher plant compartment, one of the most complex compartments in the MELiSSA loop, a Plant Characterization Unit (PCU) was recently designed and assembled on the premises of Department of Agricultural Sciences of University of Naples Federico II in Italy as part of the ESA MELiSSA PaCMan (PlAnt Characterization unit for closed life support system – engineering, MANufacturing & testing) activity (Pannico et al., 2022). The PCU is a gas-tight cultivation chamber for characterization of higher plants, offering extensive monitoring and control of the cultivation environment, including its separated hydroponic and atmospheric loops.

Lettuce is a highly relevant species for bioregenerative life support systems with high harvest index, efficiency (per area, time, and volume), and potential yield (edible biomass, $O_2$ and water), combined with relatively modest horticultural requirements (Berkovich et al., 2004). Lettuce has been successfully cultivated onboard the International Space Station (Khodadad et al., 2020) and represents a healthy and nutritious addition to the human diet, rich in vitamin C, antioxidants, polyphenols and dietary fiber (Khodadad et al., 2020). Furthermore, it is one of the most used vegetables in terrestrial hydroponic cultivation systems (Zhu et al., 2020), illustrating the benefits of a deeper understanding of plant responses to nutrient solutions derived from organic waste in commercial crop production also on Earth, with the potential to improve resource utilization and reduce environmental impact of industrial food production systems.

The underlying hypotheses and scenario of this study was that strategies and operating conditions of upstream waste processing will affect the composition of the mineralized nutrients fed to the plants in a life support system. As these strategies and conditions may be designed and controlled, but also give rise to fluctuations and dynamics, it is critical to understand and predict consequences of nutrient solution composition on crop cultivation. More specifically, urine ammonification and nitrification may result in nutrient solutions with varying concentrations of $NH_4^+$ and $NO_3^-$, including their relative ratio, which will impact downstream crop

cultivation. Furthermore, beyond the incoming nutrient streams, nutrient utilization rates inside the plant compartment will dictate the evolution of the nutrient solution in a closed-loop scenario with complete recycling of water, nutrients and non-nutrients. This study aimed at investigating biological and system effects of high and low $NH_4^+$:N ratios on lettuce cultivated in a urine recycling scenario, exploiting the recently established PCU facility offering controlled hydroponic cultivation conditions and state of the art monitoring of critical parameters such as $O_2$ production.

# 2 Materials and methods

## 2.1 Lettuce seedling production

About 100 lettuce seeds (*Lactuca sativa* L. cultivar 'Grand Rapids') were disinfected in 5% sodium hypochlorite solution for 15 minutes followed by three rinsing cycles in ultrapure water. The disinfected seeds were dispersed onto absorbent paper, moist with ultrapure water and incubated at room temperature under indirect lighting. After 48 hours, germinated seeds with about 1 cm radicle were transferred to Styrofoam trays with vermiculite soaked in nutrient solution prepared according to Peiro et al. (2020) at 0.5X strength, and incubated at 24°C in a dedicated nursery with 65% relative humidity (RH), a light/dark regime of 16/8 hours and a light intensity of 400 ± 50 µmol·m$^{-2}$·s$^{-1}$ (PPFD). Ten days after sowing, 18 equally developed seedlings (evaluated by visual inspection) were selected from the pool of 100 germinated seeds. Each seedling was installed into a bottomless 50 mL test tube (CLS430829, Corning, NY, USA) filled with rockwool (Delta 4G 42/40, Grodan, Roermond, The Netherlands) cut into a cylindrical shape and vertically split in two. The seedling's root system was sandwiched between the two halves of the rockwool column and inserted into the 50 mL tube. The top surface of the rockwool was then covered with grafting mastic (Cortimax, Cisa Adriatica S.r.l., Pescara, Italy) to minimize gas exchange between the root and shoot zones of the cultivation chamber.

## 2.2 Cultivation chamber and cultivation conditions

For each of the two crop tests (designated HiNH$_4^+$ and LoNH$_4^+$), 18 lettuce plants were cultivated inside the PCU. Within one crop test, all plants shared the same nutrient solution (recirculated within the PCU's hydroponic loop) and the same atmosphere (recirculated within the PCU's atmospheric loop). The plants were cultivated for 28 days inside the PCU chamber to a total plant age of 38 days. The day/night cycle was 16/8 hours, with an average light intensity across the plant positions of 430 µmol·m$^{-2}$·s$^{-1}$ (PPFD represented by 23% blue, 20% green and 57% red light). PPFD and spectral composition were recorded by eighteen spectral scans (one per plant position, measured at a height of 3 cm above the medium surface) using a spectral radiometer (MSC15, Gigahertz-Optik, Türkenfeld, Germany). The largest deviation between this average light intensity and the intensity at any of the

plant positions was 68 µmol·m$^{-2}$·s$^{-1}$ (PPFD), corresponding to 16% of the average intensity. The air temperature and RH were automatically controlled as described by Pannico et al. (2022), at 26°C and 50% during the day and 20°C and 70% during the night, respectively. The atmospheric $CO_2$ concentration was controlled at 1000 ppmv (parts per million by volume) by automatic injection of pure $CO_2$ during the day phase, while it was allowed to increase during the night phase due to respiration. Atmospheric $O_2$ concentration started at ambient levels and increased based on plant photosynthesis. The atmospheric $O_2$ concentration was not controlled beyond one chamber venting per crop test (Day 19) to avoid $O_2$ levels rising above 25%.

## 2.3 Nutrient solution preparation, monitoring, and maintenance

The nutrient solutions were based on the recipe described by Peiro et al. (2020) with the exception of i) the $NH_4^+$:N ratio was either reduced (LoNH$_4^+$ crop test) or increased (HiNH$_4^+$ crop test) using $SO_4^{2-}$ as counter-ion for required charge balancing, and ii) Na$^+$ and Cl$^-$ levels were increased (both crop tests). Identification of prioritized nutrient solutions for the two PCU crop tests was based on preliminary deep water crop cultivation experiments with various $NH_4^+$:N ratios (0.00, 0.11, 0.22, 0.44, 0.50 mol·mol$^{-1}$), nutrient solution strengths (0.75, 1.00, 1.25 X) and NaCl concentrations (0, 5 mM). PCU crop cultivation conditions were selected aiming at the presence of NaCl (5 mM) to mimic a urine recycling scenario (see Results section), reduced nutrient solution strength (0.75 X) to minimize negative effects of elevated total ionic strength (maintaining same electrical conductivity for the LoNH$_4^+$ crop test as for the nutrient solution of Peiro et al. (2020), 1.9 mS/cm), and two $NH_4^+$:N ratios representing considerable differences (high and low) while still providing acceptable plant growth conditions and representing relevant degrees of nitrification in a BLSS perspective (see Results section). The nutrient solutions of the LoNH$_4^+$ and HiNH$_4^+$ crop tests were obtained by mixing the following A and B stock solutions made from reverse osmosis water: LoNH$_4^+$ Stock A consisted of 434 mM Ca(NO$_3$)$_2$, 90 mM CaCl$_2$, 9.6 mM FeCl$_3$ and 12 mM Na-EDTA. HiNH$_4^+$ Stock A consisted of 213 mM Ca(NO$_3$)$_2$, 311 mM CaCl$_2$, 9.6 mM FeCl$_3$ and 12 mM Na-EDTA. LoNH$_4^+$ Stock B consisted of 120 mM MgSO$_4$, 420 mM KNO$_3$, 180 mM KH$_2$PO$_4$, 207 mM NH$_4$NO$_3$, 187 mM NaNO$_3$, 590 mM NaCl, and micronutrients. HiNH$_4^+$ Stock B consisted of 120 mM MgSO$_4$, 420 mM KNO$_3$, 415 mM (NH$_4$)$_2$SO$_4$, 180 mM KH$_2$PO$_4$, 107 mM NH$_4$NO$_3$, 315 mM Na$_2$SO$_4$, 145 mM NaCl, and micronutrients. Micronutrients (part of Stock B) were 2.4 mM H$_3$BO$_3$, 0.42 mM ZnSO$_4$, 96 µM CuSO$_3$, 0.6 mM MnSO$_4$, and 60 µM H$_2$MoO$_4$. For the LoNH$_4^+$ crop test, LoNH$_4^+$ A and B stock solutions were added at a 1:1 ratio to achieve an electrical conductivity of 1.9 mS·cm$^{-1}$ at startup, similar to that of Peiro et al. (2020). This resulted in a total N concentration of 11 mM. For the HiNH$_4^+$ crop test, HiNH$_4^+$ A and B stock solutions were added at a 1:1 ratio to achieve the same total N concentration (11 mM). This resulted in an electrical conductivity of 2.2 mS·cm$^{-1}$ at startup, due to higher concentrations of $SO_4^{2-}$ used for charge balancing. The measured ion concentrations, pH and EC of

both nutrient solutions are summarized in Table 1. The total liquid volume in the hydroponic loop was 265 - 275 L throughout both crop tests.

Water quality of the recirculating nutrient solution was continuously monitored, including pH (2 x Endress+Hauser Orbisint CPS11D Memosens, Germany), electrical conductivity (EC; 2 x Endress+Hauser Indumax CLS50D, Germany), dissolved $O_2$ (Mettler Toledo InPro 6860i, Switzerland), dissolved $CO_2$ (Labolytic optical $CO_2$ sensor 0-15 mg/L, Trondheim, Norway), and nitrate (Endress+Hauser Viomax CAS51D, Germany, installed in an at-line configuration with auto-sampling and auto-dilution of the nutrient solution). Nutrient solution temperature was continuously monitored and automatically controlled at 18 ± 0.5°C. For both crop tests, pH was adjusted to 5.9 at startup using 0.5 M $H_2SO_4$ and then maintained at 5.9 by automatic addition of 0.5 M KOH throughout both crop tests (no addition of acid necessary during the cultivation period). Throughout both crop tests, the actual pH of the nutrient solution typically deviated less than 0.05 pH units from the set-point, and never more than 0.2 pH units. During both crop tests, nutrient stock solutions A and B were automatically fed at a 1:1 ratio to maintain a constant $NO_3^-$ concentration. The recirculating nutrient solution was mechanically filtered in three steps with reducing pore size from 1.6 to 0.45 μm, using filter cartridges (PP3 Sartopure - Sartobran, Sartorius, Goettingen, Germany). The filtration unit was implemented between the plant cultivation chamber and the stirred tank holding the nutrient solution that was continuously fed to the plants.

## 2.4 Data collection, sampling, and analysis

Atmospheric concentrations of $O_2$ and $CO_2$ inside the cultivation chamber were continuously measured by an $O_2/CO_2$ gas analyzer (California Analytical Instruments, 700 LX NDIR/$O_2$, Orange, CA, USA). Additionally, the $O_2$ and $CO_2$ concentrations of the pressure compensation system's gas tank were measured at crop test start and end, and before and after chamber venting. The amount of atmospheric gas inside the PCU was determined continuously based on ideal gas law, a total atmospheric volume of 4.9 $m^3$, and continuously measured gas pressure and temperature. This allowed computation of daily atmospheric leak rates and plant $O_2$ production (Pannico et al., 2022). To keep the air humidity constant, the water produced by the plant transpiration was condensed and collected (Pannico et al., 2022). During the crop tests presented in this study, the injection rates of $CO_2$ and water into the atmospheric loop were inaccurate, unfortunately preventing accurate mass balances for $CO_2$ and water and thereby also preventing calculation of consumed amounts of $CO_2$ and produced amounts of water.

TABLE 1 Characterization of the $LoNH_4^+$ and $HiNH_4^+$ nutrient solutions at start (0 days after transplant (DAT)) and end (28 DAT) of each crop test.

| | $LoNH_4^+$ | | $HiNH_4^+$ | |
|---|---|---|---|---|
| | 0 DAT | 28 DAT | 0 DAT | 28 DAT |
| $NO_3^-$ [mM] | 9.7 | 9.7 | 5.6 | 5.6 |
| $NH_4^+$ [mM] | 1.3 | 0.2 | 5.3 | 1.6 |
| $NO_2^-$ [mM] | 0.0 | 0.0 | 0.0 | 0.5 |
| Total N [mM] | 11.0 | 10.0 | 10.9 | 7.8 |
| $HPO_4^{2-}$ [mM] | 0.8 | 0.7 | 0.9 | 0.7 |
| $K^+$ [mM] | 3.7 | 3.1 | 3.5 | 7.4 |
| $Ca^{2+}$ [mM] | 4.6 | 6.5 | 4.8 | 4.6 |
| $Mg^{2+}$ [mM] | 0.7 | 0.8 | 0.7 | 0.6 |
| $SO_4^{2-}$ [mM] | 0.8 | 0.9 | 4.9 | 4.7 |
| $Cl^-$ [mM] | 4.5 | 5.2 | 4.7 | 4.2 |
| $Na^+$ [mM] | 5.1 | 6.4 | 4.9 | 4.8 |
| $NH_4^+:NO_3^-$ [mol·mol$^{-1}$] | 0.14 | 0.03 | 0.95 | 0.28 |
| $NH_4^+:N$ [mol·mol$^{-1}$] | 0.12 | 0.02 | 0.49 | 0.20 |
| Na:N [mol·mol$^{-1}$] | 0.46 | 0.64 | 0.46 | 0.62 |
| Cl:N [mol·mol$^{-1}$] | 0.41 | 0.52 | 0.43 | 0.54 |
| K:N [mol·mol$^{-1}$] | 0.33 | 0.31 | 0.32 | 0.96 |
| pH | 5.9 | 5.9 | 5.9 | 5.9 |
| EC [mS·cm$^{-1}$] | 1.9 | 1.9 | 2.2 | 2.3 |

Top-view images of the 1.2 m × 1.5 m cultivation chamber floor were acquired every hour (FLIR Blackfly S BFS-U3-200S6C-C @ 70 dpi), and projected leaf area as observed from above was calculated for images acquired every second day based on image segmentation by color. Projected Leaf Area Index (PLAI) was calculated as the measured projected leaf area of all 18 plants (m$^2$) per total cultivation area (m$^2$) (Zheng and Moskal, 2009). SPAD index for indication of chlorophyll content (average of ten measurements per plant; SPAD-502, Minolta Corp. Ltd, Osaka, Japan), dark-adapted chlorophyll fluorescence for the maximum quantum yield of photosystem II ($F_v/F_m$) (average of two measurements per plant; Plant Stress Kit, Opti-Sciences), and leaf color index (average of three measurements per plant; Chroma Meter CR-400, Konika Minolta) were measured immediately after opening the cultivation chamber at day of harvest. Fresh weight of shoot and stem, and leaf number were determined for each plant by destructive sampling. Additionally, total leaf area of each plant was determined from top-view images of the plant's individual leaves (Canon EOS 90D + Tamron SP 35 mm @ 59 dpi) based on image segmentation by color.

The lead taproot of each plant was isolated and imaged (Canon EOS 90D + Tamron SP 35 mm @ 294 dpi for LoNH$_4^+$ and 334 dpi for HiNH$_4^+$) in a tray with water. The lead taproot was defined as the medial root with the largest diameter in the basal zone, not considering the diameter of the laterals. Root length, diameter and number of links and forks were analyzed with WinRhizo (Pro 2021a, Regent Instruments Inc.). Following counting of leaf number and determination of shoot fresh weight (FW) of each plant, shoots and roots were oven-dried at 60°C until constant weight was reached for determination of dry weight (DW) per plant. Total plant DW was calculated as shoot DW + root DW, while harvest index was calculated as shoot DW per total plant DW. Dried samples of shoots and roots were analyzed for total carbon (C) and N content via combustion analysis by a Micro Elemental Analyser UNICUBE$^{\circledR}$ (Elementar, Langenselbold Hesse, Germany) equipped with a thermal conductivity detector. Leaf soluble cations and anions were determined by liquid ion exchange chromatography (ICS-3000, Dionex, Sunnyvale, CA, USA) as described by Pannico et al. (2019).

Every two days, nutrient solution samples (25 mL) were extracted from the hydroponic loop for offline analysis. Nutrient ion concentrations were determined by ion exchange chromatography (ICS 3000 Dionex) and the results were smoothed by moving average to filter out noise from analysis uncertainty. N mass balance was calculated based on measured parameters at the start and end of each crop test, including concentrations of inorganic N in the nutrient solution (measured via optical sensor and ion chromatography methods described above), total liquid volume, total shoot and root biomass and their N content, in addition to the amount of nutrient stock solutions introduced and samples removed throughout the crop test.

Statistical analyses were performed with SPSS (IBM SPSS version 28.0.0.0), Anova with Tukey HSD post-test, tests of normality, Independent Samples t-test and Mann Whitney U test.

# 3 Results

Building on the background presented in the introduction, the results section first presents the experiment rationale with respect to nutrient solution composition and cultivation conditions. Representing the first scientific paper detailing crop cultivation results from the recently established PCU facility, plant growth and selected scientific datasets offered by this facility are then illustrated on a high level, before being explored in more detail to present effects of crop cultivation in low vs. high NH$_4^+$:N ratio.

## 3.1 Urine recycling scenario: Experiment rationale and nutrient solution design

The experiment rationale was built on the hypothesis presented in the introduction that both design and natural dynamics of upstream waste processing may result in mineralized waste streams with different NH$_4^+$:NO$_3^-$ ratios, which in turn may affect the biology of a downstream plant compartment and thus the overall BLSS performance. Effects of different NH$_4^+$:NO$_3^-$ ratios in the nutrient solution were explored in a mineralized urine scenario, using NH$_4^+$ and NO$_3^-$ as the sole N sources. Two crop tests (two treatments), designated LoNH$_4^+$ and HiNH$_4^+$, were performed with NH$_4^+$ to total N ratios (NH$_4^+$:N) of 0.1 and 0.5 mol·mol$^{-1}$, respectively. Relating to a foreseen upstream nitrification process, the LoNH$_4^+$ scenario (0.1 mol·mol$^{-1}$ NH$_4^+$:N) represents nearly complete nitrification, while the HiNH$_4^+$ scenario (0.5 mol·mol$^{-1}$ NH$_4^+$:N) represents nitrification without increased alkalinity and thus limited by redox, as reviewed by Larsen et al. (2021). At the same time, these scenarios represent considerable different, low and high NH$_4^+$:N ratios for lettuce cultivation (Zhu et al., 2020; Du et al., 2022; Hameed et al., 2022) while still avoiding the use of NH$_4^+$ as the dominant N source to limit the potential of ammonium toxicity and thereby allow acceptable growth (see Materials and methods). To allow direct comparison of results, total N concentration was identical at startup of both crop tests (11 mM). Capitalizing on a state-of-the-art nutrient monitoring and control system, the NO$_3^-$ concentration was kept constant (9.7 mM in LoNH$_4^+$; 5.6 mM in HiNH$_4^+$) throughout each of the two crop tests to minimize effects of the absolute NO$_3^-$ concentration itself. This allowed the NH$_4^+$:N ratio to change throughout the cultivation period depending on the total consumption of NH$_4^+$ and NO$_3^-$ in the system, demonstrating the development of the NH$_4^+$:N ratio over time.

In line with a urine recycling scenario, the crop tests were performed with an elevated NaCl concentration of 5 mM, representing a Na:N concentration ratio of 0.46 mol·mol$^{-1}$. This ratio was designed based on typical Na:N ratios of mineralized urine. While fresh urine is typically characterized by 0.17 mol·mol$^{-1}$ Na:N and Cl:N (adapted from Udert et al., 2006), several reports illustrate ratios of approximately 0.25 mol·mol$^{-1}$ in urine-based fertilizer solutions (adapted from Bonvin et al., 2015; Mauerer et al., 2018; Halbert-Howard et al., 2021). However, the final composition of the mineralized nutrient solutions depends on urine storage and ammonification and nitrification processes. As urine is prone to

ammonia volatilization, resulting Na:N and Cl:N ratios may be considerably elevated - exemplified by the real stored urine fraction by Udert and Wachter (2012) with Na:N and Cl:N ratios of 0.5 mol·mol^{-1}. Thus, the Na:N and Cl:N concentration ratios used in this study represent a urine-based nutrient solution, accounting for effects by urine storage and processing. However, effects of potential Na^{+} accumulation over time in a closed loop system are not accounted for in this study, as such predictions would benefit from more insight in Na uptake ratios as function of nutrient solution composition and cultivation conditions.

Beyond $NH_4^+/NO_3^-$ and $Na^+/Cl^-$, the two crop tests were run with similar concentrations of macro- and micronutrients, except for $SO_4^{2-}$ used for charge balancing of $NH_4^+/NO_3^-$. The total strength of the nutrient solutions was designed so that the total electrical conductivity of the $LoNH_4^+$ nutrient solution at start was identical to that of Peiro et al. (2020) (1.9 mS·cm^{-1}) used for similar MELiSSA studies of hydroponic lettuce cultivation (resulting in an electrical conductivity of 2.2 mS·cm^{-1} for the $HiNH_4^+$ nutrient solution due to the elevated requirement of $SO_4^{2-}$ for charge balancing). The resulting nutrient solutions based on the above design criteria are illustrated in Table 1.

## 3.2 Crop cultivation in the ESA MELiSSA Plant Characterization Unit

The results reported in this paper were obtained in the recently established ESA MELiSSA Plant Characterization Unit (PCU), in which 18 lettuce plants were hydroponically cultivated as deep-water culture for 28 days after transplant (DAT), to a total age of 38 days, across a 1.8 m[2] plant cultivation area (Figure 1). Extensive monitoring and control systems provided stable cultivation conditions, including atmospheric temperature and RH, and nutrient solution temperature, pH and $NO_3^-$ concentration (see Materials and methods, Table 1; Figure 3). The closed nature of the atmospheric loop combined with continuous monitoring of atmospheric $O_2$ and $CO_2$ concentrations represent the basis for determination of $O_2$ production and $CO_2$ consumption by the plants. Atmospheric leak rates in percent gas volume per hour were calculated daily and demonstrated a stable and high system tightness with an average leak rate of 0.082 ± 0.017%·h^{-1} and 0.095 ± 0.022%·h^{-1} for the $LoNH_4^+$ and $HiNH_4^+$ crop tests, respectively. The atmospheric $O_2$ concentration increased during the day phase resulting from photosynthesis, while it decreased during the night phase due to respiration (Figure 2). As the $O_2$ production during the day phase exceeds the $O_2$ consumption during the night phase, atmospheric $O_2$ gradually increased throughout the crop tests creating a need to vent the cultivation chamber to stay below 25% $O_2$ for safety reasons (performed at Day 19 for both crop tests). Atmospheric $CO_2$ was controlled at a minimum of 1000 ppm during the day phase, while it increased due to respiration during the night phase (up to 2140 ppm during the $LoNH_4^+$ crop test). As the PCU chamber is sealed and only opened for venting and reduction of atmospheric $O_2$ concentration, sampling or physical inspection of the plants is not possible during a crop test. To demonstrate biomass development, Projected Leaf Area Index (PLAI) was calculated based on top-view images acquired by the PCU's internal color camera (Figure 4). To further indicate differences

in biomass development over time (Figure 4) despite the lack of true biomass measurements, PLAI was used as a basis for calculating a specific growth rate, here introduced as $\mu_{PLAI}$, according to Equation 1 where t symbolizes time (in DAT).

$$\mu_{PLAI} = \frac{\frac{d(PLAI)}{d(t)}}{PLAI} \qquad \text{Equation 1}$$

## 3.3 Plant development and physiology at high and low $NH_4^+:NO_3^-$ ratios

### 3.3.1 Shoot development over time as observed by non-destructive methods

A relatively stable $\mu_{PLAI}$ during the first 16 - 18 days indicates close to exponential growth for plants in both the $HiNH_4^+$ crop test and the $LoNH_4^+$ crop test in this period. From approximately 20 DAT, as the plants mature and start to overlap, the PLAI-based specific growth rates of both treatments coincide and decrease (Figure 4). Regression analysis of PLAI from 0 to 16 DAT was performed using exponential trendlines (Figure 4; $R^2$ factors > 0.999), demonstrating a reduced $\mu_{PLAI}$ for plants growing in the $HiNH_4^+$ nutrient solution (0.18 per day) compared to that of $LoNH_4^+$ (0.22 per day). The initial PLAI of $HiNH_4^+$ and $LoNH_4^+$ plants were similar due to identical germination and seedling phases (both 0.010 m[2]·m^{-2} at 2 DAT). The final PLAI of the $LoNH_4^+$ crop test at 28 DAT reached 0.70 m[2]·m^{-2} corresponding to a projected leaf area of 1.3 m[2], while corresponding values of $HiNH_4^+$ were 44% lower with 0.39 m[2]·m^{-2} PLAI and 0.71 m[2] projected leaf area. Closer inspection of the PLAI of the two crops illustrate that their differences stayed below approximately 20% during the first 10 days in the PCU, before it increased gradually up to approximately 45% at 18 DAT and remained at this level throughout the rest of the cultivation period.

### 3.3.2 Root and shoot biomass and morphology at harvest

In line with the differences demonstrated by non-destructive PLAI analysis, detailed inspection of the plants after destructive sampling at 28 DAT illustrated a total leaf area of the $HiNH_4^+$ crop which was 50% lower than that of the $LoNH_4^+$ crop (3.5 m[2] vs. 7.0 m[2], respectively, for the 18 plants; Table 2). The results demonstrate that the shoot biomass was affected in a similar way, with the $HiNH_4^+$ plants having 58% lower shoot fresh weight and 40% lower shoot dry weight compared to the $LoNH_4^+$ plants. The difference in these numbers illustrate a higher shoot dry weight content of the $HiNH_4^+$ plants compared to the $LoNH_4^+$ plants (10% vs. 7%, respectively). Furthermore, the $HiNH_4^+$ plants developed a significantly lower number of leaves (35%) compared to the $LoNH_4^+$ group.

The dry root biomass difference between the two crops (19% lower for $HiNH_4^+$ plants) was smaller than the shoot dry biomass difference (40% lower for $HiNH_4^+$), illustrating a higher root:shoot ratio and a lower harvest index of the $HiNH_4^+$ plants compared to those of $LoNH_4^+$ (Table 2). Following harvest and destructive sampling, the lead taproot of each plant (see Materials and methods) was isolated, imaged, and analyzed. The taproots of the $HiNH_4^+$ and $LoNH_4^+$ plants demonstrated considerable differences,
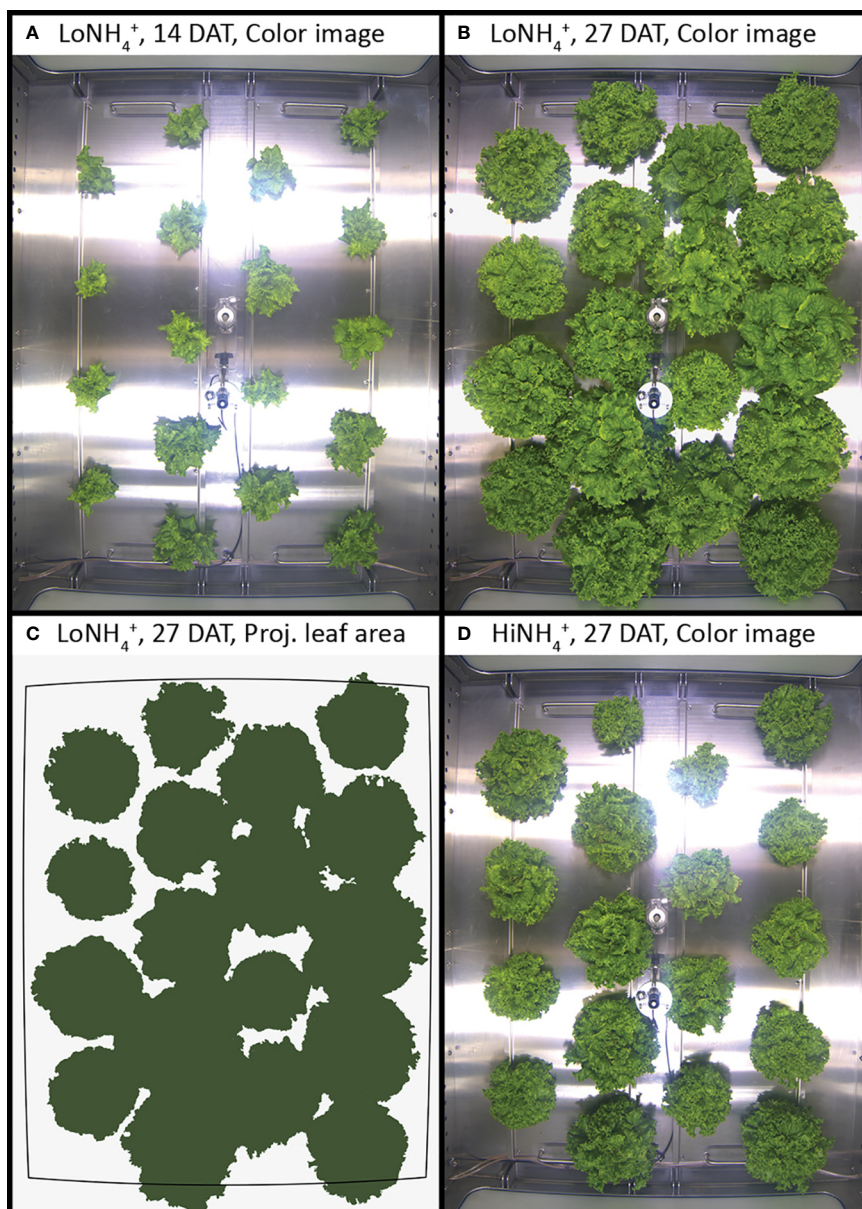
FIGURE 1
Top-view color images of lettuce inside the PCU cultivation chamber at 14 and 27 days after transplant (DAT), cultivated in LoNH$_4^+$ **(A, B)** and HiNH$_4^+$ nutrient solution **(D)**. Example illustrating image segmentation for determination of projected leaf area **(C)**.

as qualitatively indicated in Figure 5. In average, the lead taproots of HiNH$_4^+$ were shorter (55% reduction in total length, including both mother root and lateral roots), thinner (15% reduction in average diameter) and less branched (57% less forks) than those of the LoNH$_4^+$ plants.

### 3.3.3 Leaf chlorophyll content, color index and F$_v$/F$_m$ at harvest

Dark-adapted chlorophyll fluorescence measurements of the maximum quantum yield of photosystem II (F$_v$/F$_m$) were identical for both treatments (Table 3), while an elevated SPAD index indicated a higher chlorophyll content of the leaves of the HiNH$_4^+$ plants. Color measurements illustrated significant

differences as evaluated by the L*a*b color space, with the HiNH$_4^+$ leaf color shifted more towards green compared to the color of the LoNH$_4^+$ leaves.

### 3.3.4 Nutrient ion and element composition of shoots and roots at harvest

Nutrient ion and element analyses of lettuce shoot and root biomass harvested at 28 DAT demonstrated considerable differences between plants cultivated in the two different nutrient solutions (Table 4). The biomass content of NO$_3^-$ and NH$_4^+$ varied in line with their concentrations and ratios in the nutrient solutions. The HiNH$_4^+$ plants exhibited an NH$_4^+$ root content nearly three
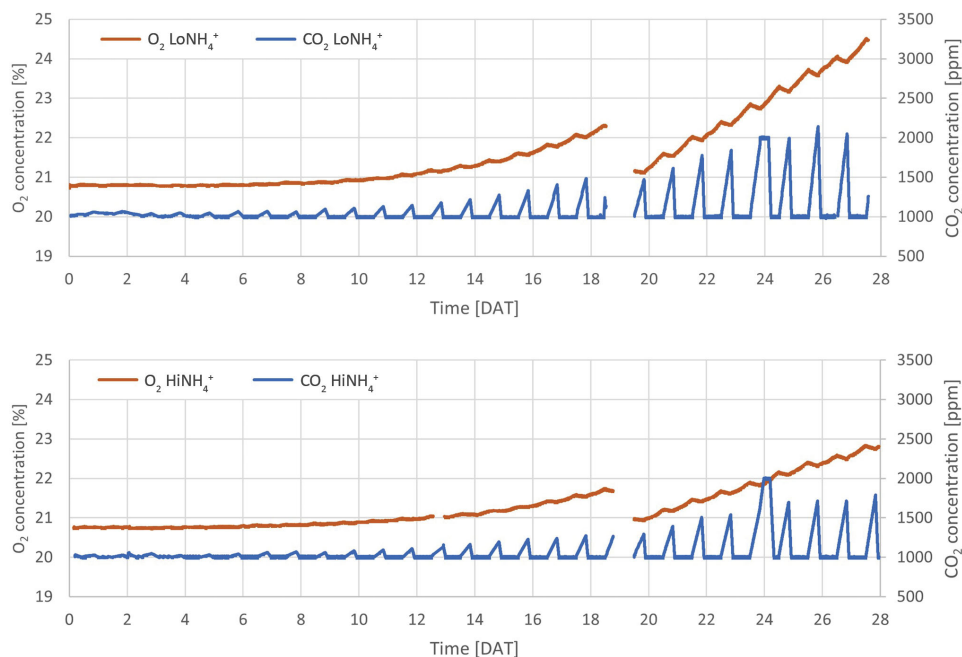
**FIGURE 2**
Absolute concentrations of atmospheric $O_2$ and $CO_2$ throughout the $LoNH_4^+$ (upper graph) and $HiNH_4^+$ (lower graph) crop tests. Missing data from 19 DAT represents a venting event in which the cultivation chamber was opened to reduce the $O_2$ concentration.

times higher and a $NO_3^-$ shoot and root content 7 – 8 times lower than that of the $LoNH_4^+$ plants. Considering total N, the most significant differences were observed for the roots, for which the total N content was 28% higher in the $HiNH_4^+$ plants. Additionally, the C content of $HiNH_4^+$ plants was higher than that of the $LoNH_4^+$

plants (9% higher in shoot content and 15% higher in root content). The content of other nutrient ions was generally lower in plants cultivated in $HiNH_4^+$ nutrient solution compared to those cultivated in $LoNH_4^+$. This includes the cations $K^+$ (52% lower shoot content and 36% lower root content), $Na^+$ (32% lower shoot
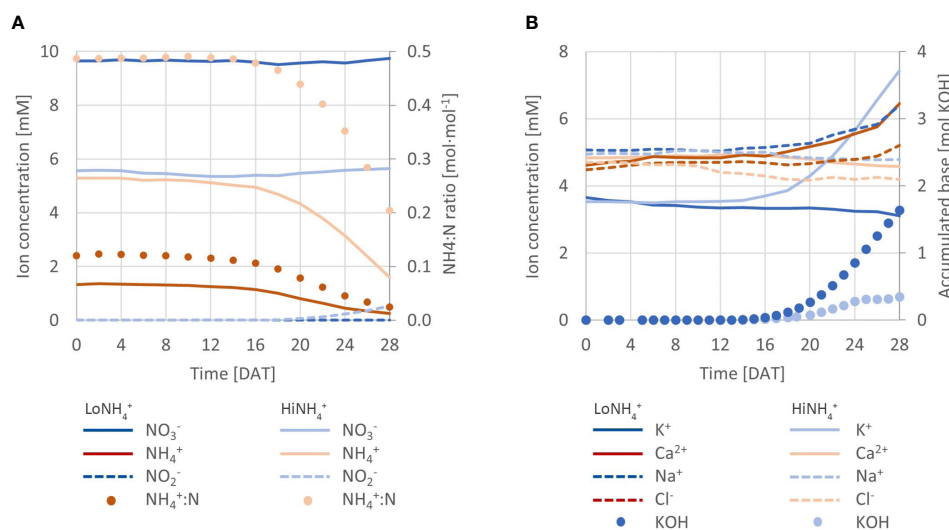


**FIGURE 3**
**(A)** Measured concentration of $NO_3^-$, $NH_4^+$, and $NO_2^-$ throughout the $LoNH_4^+$ and $HiNH_4^+$ crop tests (lines; left Y-axis), in addition to the ratio of $NH_4^+$ to total N ($NH_4^+$:N; dots; right Y-axis). **(B)** Development of $K^+$, $Ca^{2+}$, $Na^+$ and $Cl^-$ concentrations in the nutrient solutions of both crop test (lines; left Y-axis), in addition to accumulated addition of base (KOH; dots; right Y-axis).
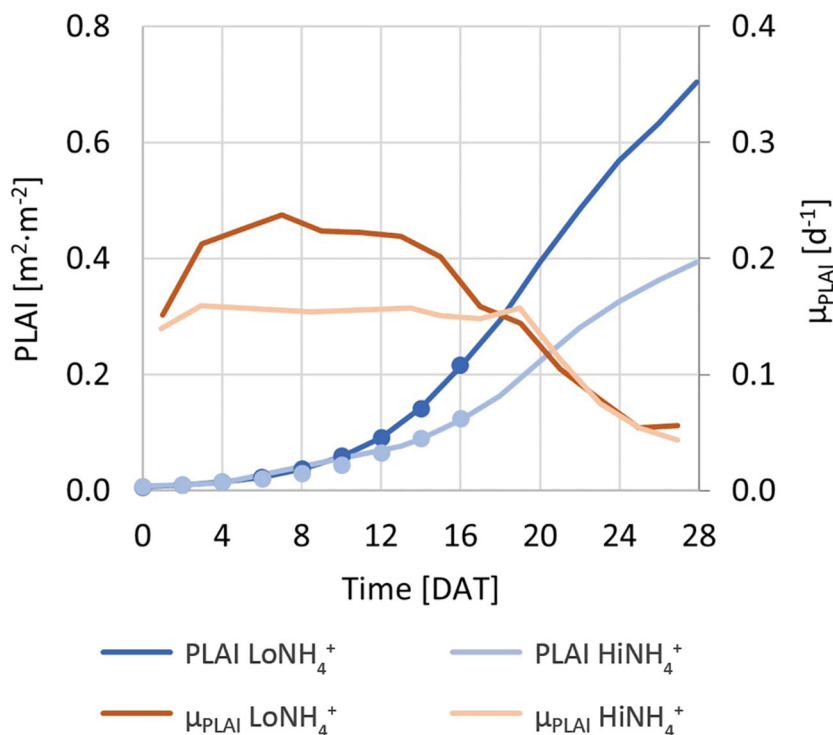
**FIGURE 4**
Blue solid lines (left Y-axis): PLAI (Projected Leaf Area Index) of the $LoNH_4^+$ and $HiNH_4^+$ crop tests. Blue circles (left Y-axis): Trendlines based on exponential regression of a subset of the PLAI dataset from 0 to 16 DAT (coinciding with the PLAI dataset in blue solid lines). Red lines (right Y-axis): PLAI-based specific growth rate, $\mu_{PLAI}$, of the $LoNH_4^+$ and $HiNH_4^+$ plants.

content and 22% lower root content), and $Mg^{2+}$ (47% lower shoot content). $Ca^{2+}$ illustrated the same trend (55% lower shoot content and 17% lower root content in $HiNH_4^+$) although the differences were not statistically significant due to high variability in the results. Reduced nutrient ion content of $HiNH_4^+$ plants could also be observed for the anions $HPO_4^{2-}$ (44% lower shoot content) and $Cl^-$ (72% lower root content), while no statistically significant differences could be observed for $SO_4^{2-}$.

## 3.4 Crop performance and system dynamics at high and low $NH_4^+$:$NO_3^-$ ratios

### 3.4.1 $O_2$ production

Continuous monitoring of the atmospheric $O_2$ and $CO_2$ concentrations inside the cultivation chamber illustrated $O_2$ production during the day (when $CO_2$ was controlled at 1000 ppm by automatic $CO_2$ injection), and $O_2$ consumption and $CO_2$

**TABLE 2** Biomass characteristics of plants from the $LoNH_4^+$ and $HiNH_4^+$ crop tests, measured at harvest (28 DAT).

| | $LoNH_4^+$ | $HiNH_4^+$ | Statistical significance |
|---|---|---|---|
| Shoot fresh weight per plant [g] | 289 ± 122 | 121 ± 51 | p < 0.01 |
| Shoot dry weight per plant [g] | 19 ± 5 | 11 ± 4 | p < 0.01 |
| Shoot dry weight content [%] | 6.9 ± 1.3 | 9.8 ± 1.6 | p < 0.01 |
| Root dry weight per plant [g] | 2.4 ± 0.7 | 1.9 ± 0.6 | p < 0.05 |
| Total dry weight per plant [g] | 21 ± 6 | 13 ± 4 | p < 0.01 |
| Harvest index | 0.88 ± 0.02 | 0.85 ± 0.02 | p < 0.01 |
| Root:shoot ratio | 0.14 ± 0.02 | 0.19 ± 0.03 | p < 0.01 |
| Stem diameter per plant [mm] | 18 ± 3 | 15 ± 3 | p < 0.01 |
| Leaf number per plant | 40 ± 19 | 26 ± 8 | p < 0.05 |
| Total leaf area per plant [$cm^2$] | 3907 ± 724 | 1961 ± 712 | p < 0.01 |

All values are tabulated as mean value ± standard deviation based on separate analyses of 18 individual plants from each crop test. Statistical significance between the two crop tests is indicated as p-values. The shoot dry weight content was calculated as shoot dry weight divided by shoot fresh weight, the harvest index was calculated as shoot dry weight divided by total dry weight, while the root:shoot ratio was calculated based on dry weight.
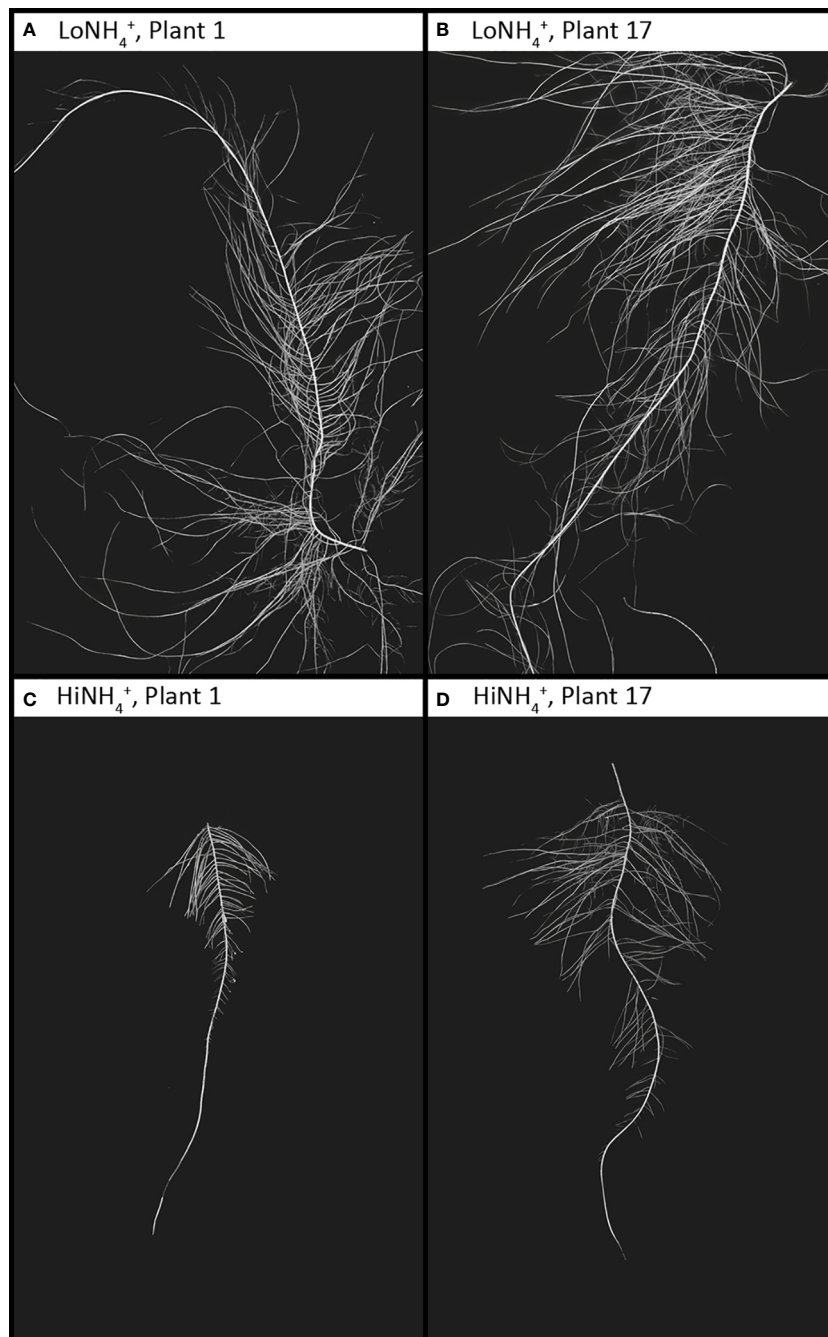
**FIGURE 5**
Lead taproots of two example $LoNH_4^+$ plants **(A, B)** and two $HiNH_4^+$ plants **(C, D)** from harvest at 28 DAT. All images are represented at the same resolution, covering a 20 x 30 cm area. Root and background contrast and color levels have been modified from the raw images to enhance root morphology.

production during the night (Figure 2). Detailed inspection of the datasets illustrates an immediate increase in atmospheric $CO_2$ concentration and a corresponding decrease in $O_2$ starting from the time at which the cultivation chamber LEDs were turned off, as illustrated in Figure 6A, detailing the first two days after the chamber venting. Reversely, an immediate decrease of $CO_2$ concentration and increase of $O_2$ was initiated when the LEDs were reactivated at the end of the night phase. During the 16-hour day phase of the 21st day (20 DAT), the $O_2$ concentration of the

cultivation chamber increased 0.48 vol-% in the $LoNH_4^+$ crop test, and 0.26 vol-% in the $HiNH_4^+$ crop test. During this day, the $LoNH_4^+$ plants covered a 0.71 $m^2$ cultivation area, while the $HiNH_4$ plants covered 0.40 $m^2$ (as evaluated by projected leaf area). During the following 8-hour night phase, the $CO_2$ concentration increased linearly to 1614 ppm ($LoNH_4^+$) and 1391 ppm ($HiNH_4^+$) (with no injection of $CO_2$). After reactivating the LEDs, the atmospheric $CO_2$ concentration returned to 1000 ppm after 1.5 hours ($LoNH_4^+$) and 1.6 hours ($HiNH_4^+$) of daylight. Corresponding analyses at the end

TABLE 3   $F_v/F_m$ (average of two measurements per plant), SPAD (average of ten measurements per plant) and Color index (average of three measurements per plant) values of the 18 $LoNH_4^+$ and 18 $HiNH_4^+$ plants as measured at harvest (28 DAT).

| Parameter | $LoNH_4^+$ | $HiNH_4^+$ | Statistical significance |
|---|---|---|---|
| $F_v/F_m$ | 0.83 ± 0.01 | 0.83 ± 0.01 | *Not sign.* |
| SPAD index | 20 ± 3 | 23 ± 2 | p < 0.01 |
| Color index L | 53 ± 3 | 51 ± 3 | *Not sign.* |
| Color index a | -18.8 ± 0.5 | -18.3 ± 0.5 | p < 0.01 |
| Color index b | 34.3 ± 1.3 | 32.6 ± 1.8 | p < 0.01 |

All values are tabulated as mean value ± standard deviation. Statistical significance between the two treatments is indicated as p-values.
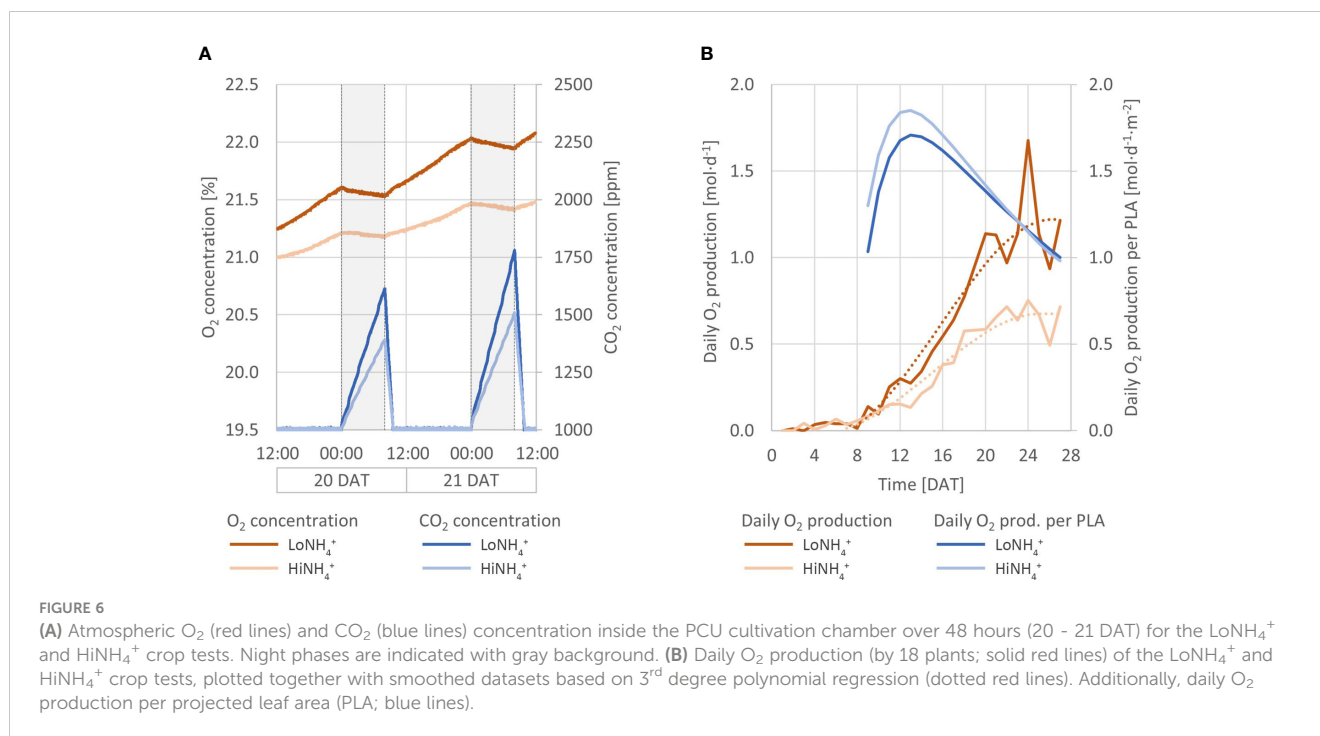
of the crop tests demonstrated an increase in $O_2$ concentration of 0.59 vol-% by the $LoNH_4^+$ plants (1.21 $m^2$ projected leaf area), and 0.33 vol-% by the $HiNH_4^+$ plants (0.71 $m^2$ projected leaf area) during the day phase of the 28th day. The total $O_2$ amount inside the PCU atmospheric loop and its pressure compensation system was precisely determined at the time of cultivation chamber closing and opening (see Materials and methods). Compensating for the accurately determined chamber gas leaks, this allows detailed calculations of the $O_2$ amount produced by the plants during the two phases of each crop test before (0 - 18 DAT) and after (20 - 28 DAT) chamber venting (totaling 26.6 days; Table 5). Considering the absolute $O_2$ production, the $HiNH_4^+$ plants produced 34% less $O_2$ during the first phase (0 - 18 DAT) and 43% less $O_2$ during the second phase (20 - 28 DAT) compared to the $LoNH_4^+$ plants.

TABLE 4   Average shoot and root nutrient ion and element content of the 18 $LoNH_4^+$ and 18 $HiNH_4^+$ lettuce plants as measured at harvest (28 DAT).

|  |  | $LoNH_4^+$ | $HiNH_4^+$ | Statistical significance |
|---|---|---|---|---|
| Shoots | Total C | 382 ± 11 | 416 ± 9 | p < 0.01 |
|  | Total N | 39 ± 7 | 34 ± 5 | p < 0.05 |
|  | $NO_3$-N | 6.0 ± 2.6 | 0.8 ± 0.3 | p < 0.01 |
|  | $NH_4$-N | 1.0 ± 0.3 | 1.1 ± 0.2 | *Not sign.* |
|  | $PO_4$-P | 4.8 ± 1.1 | 2.7 ± 0.5 | p < 0.01 |
|  | $K^+$ | 71 ± 15 | 34 ± 6 | p < 0.01 |
|  | $Ca^{2+}$ | 3.8 ± 0.7 | 1.7 ± 0.3 | *Not sign.* |
|  | $Mg^{2+}$ | 1.9 ± 0.3 | 1.00 ± 0.14 | p < 0.01 |
|  | $SO_4$-S | 1.1 ± 0.3 | 1.3 ± 0.3 | *Not sign.* |
|  | $Na^+$ | 4.6 ± 0.6 | 3.1 ± 1.4 | p < 0.01 |
|  | $Cl^-$ | 20 ± 5 | 17 ± 3 | *Not sign.* |
| Roots | Total C | 335 ± 19 | 384 ± 6 | p < 0.01 |
|  | Total N | 56 ± 2 | 72 ± 5 | p < 0.01 |
|  | $NO_3$-N | 18 ± 3 | 2.7 ± 0.6 | p < 0.01 |
|  | $NH_4$-N | 1.3 ± 0.2 | 3.5 ± 0.3 | p < 0.01 |
|  | $PO_4$-P | 13.9 ± 1.0 | 15.2 ± 1.4 | *Not sign.* |
|  | $K^+$ | 97 ± 11 | 62 ± 4 | p < 0.01 |
|  | $Ca^{2+}$ | 1.03 ± 0.17 | 0.9 ± 0.2 | *Not sign.* |
|  | $Mg^{2+}$ | 1.07 ± 0.13 | 1.20 ± 0.12 | *Not sign.* |
|  | $SO_4$-S | 8.8 ± 1.7 | 9.4 ± 0.7 | *Not sign.* |
|  | $Na^+$ | 4.7 ± 0.8 | 3.7 ± 1.0 | p < 0.01 |
|  | $Cl^-$ | 6.7 ± 1.4 | 1.9 ± 0.6 | p < 0.01 |

All values are tabulated as mean value ± standard deviation in unit g/kg dry weight based on separate analyses of individual plants. Statistical significance between the two treatments is indicated as p-values.

**FIGURE 6**
**(A)** Atmospheric $O_2$ (red lines) and $CO_2$ (blue lines) concentration inside the PCU cultivation chamber over 48 hours (20 - 21 DAT) for the $LoNH_4^+$ and $HiNH_4^+$ crop tests. Night phases are indicated with gray background. **(B)** Daily $O_2$ production (by 18 plants; solid red lines) of the $LoNH_4^+$ and $HiNH_4^+$ crop tests, plotted together with smoothed datasets based on $3^{rd}$ degree polynomial regression (dotted red lines). Additionally, daily $O_2$ production per projected leaf area (PLA; blue lines).

However, accounting for the smaller projected leaf area (PLA) of the $HiNH_4^+$ plants, average $O_2$ production per day and projected leaf area was similar for the $LoNH_4^+$ and $HiNH_4^+$ plants both during the first phase of the crop tests (1.2 vs 1.3 $mol \cdot d^{-1} \cdot m^{-2}$, respectively) and during the second phase (both 1.1 $mol \cdot d^{-1} \cdot m^{-2}$). Furthermore, relating the total $O_2$ production to the total shoot DW at harvest also demonstrates similar values for the two crops, with 37 mol $O_2$ produced (over 26.6 days) per kg shoot DW for both crops. Estimated daily $O_2$ production throughout the crop tests was calculated based on the $O_2$ concentration in the cultivation chamber, the leak rate, and estimated daily gas composition of the atmospheric pressure compensation system (see Materials and methods). As the latter introduces a modest uncertainty in the

calculations of daily $O_2$ production, the resulting datasets were smoothed by polynomial regression (Figure 6B). Evaluating the differences in daily $O_2$ production at 10, 14, 18, 22 and 26 DAT based on these datasets, the $HiNH_4^+$ plants produced 26, 37, 40, 42 and 45% less compared to the $LoNH_4^+$ plants, respectively.

To account for the considerable difference in biomass between the two treatments, the daily $O_2$ production (smoothed dataset) was evaluated per projected leaf area (PLA), measured non-destructively throughout the crop tests. These results (Figure 6B), illustrate similar daily $O_2$ productions per PLA for both treatments, with an indication of an increased $O_2$ production per PLA for the $HiNH_4^+$ plants during the early phase of the crop tests (15, 7, and 4% increase at 10, 14 and 18 DAT, respectively, and no difference

**TABLE 5** Total $O_2$ production of 18 plants during the $LoNH_4^+$ and $HiNH_4^+$ crop tests, tabulated for the cultivation periods before (18.1 days) and after (8.5 days) the chamber venting, in addition to the full crop test period (26.6 days, not accounting for the day of venting at 19 DAT).

| | Phase (duration) | $LoNH_4^+$ | $HiNH_4^+$ |
|---|---|---|---|
| Total $O_2$ production [mol] | | 3.61 | 2.40 |
| Average daily $O_2$ production [$mol \cdot d^{-1}$] | 0 - 18 DAT (18.1 days) | 0.20 | 0.13 |
| Average PLA [$m^2$] | | 0.16 | 0.10 |
| PLA-specific daily $O_2$ production [$mol \cdot d^{-1} \cdot m^{-2}$] | | 1.22 | 1.32 |
| Total $O_2$ production [mol] | | 8.74 | 4.97 |
| Average daily $O_2$ production [$mol \cdot d^{-1}$] | 20 - 28 DAT (8.5 days) | 1.03 | 0.59 |
| Average PLA [$m^2$] | | 0.97 | 0.55 |
| PLA-specific daily $O_2$ production [$mol \cdot d^{-1} \cdot m^{-2}$] | | 1.06 | 1.06 |
| Total $O_2$ production (26.6 days) [mol] | (26.6 days) | 12.4 | 7.37 |

Average daily $O_2$ production and average projected leaf area (PLA) are calculated based on the tabulated period durations, as a basis for calculation of PLA-specific daily $O_2$ production.

TABLE 6  Nitrogen (N) mass balance of the LoNH$_4^+$ and HiNH$_4^+$ crop tests.

|  | Parameter and unit | LoNH$_4^+$ | HiNH$_4^+$ |
|---|---|---|---|
| Nutrient solution | NO$_3^-$ at start [mol] | 2.66 | 1.47 |
|  | NH$_4^+$ at start [mol] | 0.36 | 1.39 |
|  | Total inorganic N at start [mol] | 3.02 | 2.87 |
|  | NO$_3^-$ addition [mol] | 0.82 | 0.03 |
|  | NH$_4^+$ addition [mol] | 0.10 | 0.03 |
|  | Total inorganic N net addition [mol] | 0.90 | 0.05 |
|  | NO$_3^-$ at end [mol] | 2.58 | 1.54 |
|  | NH$_4^+$ at end [mol] | 0.07 | 0.43 |
|  | NO$_2^-$ at end [mol] | 0.00 | 0.14 |
|  | Total inorganic N at end [mol] | 2.65 | 2.12 |
|  | Total inorganic N consumption [mol] | 1.28 | 0.80 |
| Plants | N in shoots [mol] | 1.02 | 0.53 |
|  | N in roots [mol] | 0.17 | 0.18 |
|  | N in biomass [mol] | 1.19 | 0.70 |
| Mass balance | Mass balance closure [%] | 94 | 89 |

Total inorganic N net addition accounts for addition of inorganic N (as NO$_3^-$ and NH$_4^+$) and samples removed throughout the crop tests. Mass balance closure is calculated as the amount of N in the total biomass divided by the total consumption of inorganic N.

from 20 to 28 DAT). The highest specific O$_2$ productivity (per time and PLA) estimated was 1.85 mol·d$^{-1}$·m$^{-2}$ for the HiNH$_4^+$ crop (13 DAT) and 1.71 mol·d$^{-1}$·m$^{-2}$ for the LoNH$_4^+$ crop (13 DAT).

### 3.4.2 Nutrient solution development

From start, the total N concentration was the same in both crop tests (11 mM; Table 1), while the NH$_4^+$:N ratios were different (0.1 mol·mol$^{-1}$ for LoNH$_4^+$, 0.5 mol·mol$^{-1}$ for HiNH$_4^+$). Based on an advanced PCU nutrient management system, automatic feeding of nutrient stock solutions (with the same NH$_4^+$:N ratios as from start, thus 0.1 or 0.5 mol·mol$^{-1}$, see Materials and methods) successfully maintained a constant NO$_3^-$ concentration throughout both crop tests (Figure 3A), at 9.7 mM for LoNH$_4^+$ and 5.6 mM for HiNH$_4^+$ (Table 1). While this control strategy required considerable feeding of nutrient stock solutions during the LoNH$_4^+$ crop test (0.5 L of each stock solution), practically no nutrient stock solution feeding was required during the HiNH$_4^+$ crop test (0.03 L of each), indicating a considerable NO$_3^-$ consumption during the LoNH$_4^+$ crop test, and practically no NO$_3^-$ consumption during the HiNH$_4^+$ crop test.

Without control of nutrient solution NH$_4^+$ concentration, NH$_4^+$ levels were allowed to vary based on N consumption. Throughout both crop tests, the NH$_4^+$ concentration was considerably reduced (Table 1), demonstrating a higher consumption of NH$_4^+$ relative to total N than the NH$_4^+$:N ratio of the nutrient solution. In consequence, the nutrient solution NH$_4^+$:N ratio during the LoNH$_4^+$ crop test was reduced from 0.12 to 0.02 mol·mol$^{-1}$, while it was reduced from 0.49 to 0.20 mol·mol$^{-1}$ during the HiNH$_4^+$ crop test.

Nitrite (NO$_2^-$) could not be detected (< 1 mg N L$^{-1}$) throughout the full LoNH$_4^+$ crop test and throughout the close-to-exponential phase of the HiNH$_4^+$ crop test (up to 20 DAT). During the latter test, NO$_2^-$ was detected during the last 6 days of cultivation (0.1 mM at 22 DAT, increasing to 0.5 mM at 28 DAT). To rule out major effects of nitrification on observed NH$_4^+$ consumption, operation of the cultivation facility was prolonged after removal of all plants from the system. Over the next 6 days, the NH$_4^+$ concentration decreased 0.5 mM in parallel with a further 0.4 mM increase of NO$_2^-$. Nutrient solution pH was kept constant by automatic pH control with KOH and H$_2$SO$_4$. No acid addition was required in any of the crop tests, while base addition was characterized by a considerably higher KOH consumption during the HiNH$_4^+$ crop test (1.6 mol OH$^-$) than during the LoNH$_4^+$ crop test (0.3 mol OH$^-$) (Figure 3B).

Despite no control of electrical conductivity (EC), the NO$_3^-$ based feeding of nutrient stock solutions and the pH-based feeding of base resulted in a relatively constant EC of 1.9 mS/cm during the LoNH$_4^+$ crop test and 2.2 - 2.3 mS/cm during the HiNH$_4^+$ crop test (Table 1).

Development of macronutrient concentrations (Figure 2B) in the nutrient solution was most profound for K$^+$, with a considerable increase from 3.5 to 7.4 mM during the HiNH$_4^+$ crop test (KOH was automatically added to maintain pH at setpoint). In contrast, K$^+$ concentration decreased by 0.6 mM over the LoNH$_4^+$ crop test. Other ions demonstrating a concentration change of more than 0.2 mM over the course of a crop test (beyond K$^+$ and N ion species) included Ca$^{2+}$, Na$^+$ and Cl$^-$, demonstrating an increase during the LoNH$_4^+$ crop test (requiring considerable feeding of nutrient stock

solutions) and a decrease during the HiNH$_4^+$ (conducted practically without feeding of nutrient stock solutions). For other macronutrients, including HPO$_4^{2-}$, Mg$^{2+}$, and SO$_4^{2-}$, analyses throughout the crop tests demonstrated stable levels (Table 1).

### 3.4.3 N mass balance

With a considerable nutrient solution volume (270 L), a limited cultivation area (1.8 m$^2$), and a crop with modest nutrient requirements (lettuce), mass balances are vulnerable to measurement inaccuracies especially with respect to ion concentrations in the nutrient solution. Nevertheless, a N mass balance was calculated (Table 6) based on the available datasets, demonstrating a mass balance closure of 94% (LoNH$_4^+$) and 89% (HiNH$_4^+$).

The total consumption of NO$_3^-$ and NH$_4^+$ during the LoNH$_4^+$ crop test was 0.9 and 0.4 mol, respectively, illustrating an apparent NH$_4^+$:N consumption ratio of 0.31 mol·mol$^{-1}$ during the LoNH$_4^+$ crop test. In contrast, with no observed consumption of NO$_3^-$ during the HiNH$_4^+$ crop test, N consumption was apparently based on NH$_4^+$ only. Relative to the produced biomass (Table 2), the consumption of inorganic N (Table 6) was 3.1 mol·kgDW$^{-1}$ for both crop tests.

### 3.4.4 Incorporation of C and N into edible biomass

To illustrate C and N recycling in a BLSS perspective, the amounts of C and N incorporated into edible biomass (18 plants per crop) was calculated for both crop tests (Figure 7) based on measured shoot DW at harvest (Table 2), and their composition (Table 4). The edible biomass of the HiNH$_4^+$ crop (202 g DW) was 40% lower than that of the LoNH$_4^+$ crop (337 g DW), while the relative shoot C content of the HiNH$_4^+$ crop (42%) was higher than that of the LoNH$_4^+$ crop (38%). In sum, the HiNH$_4^+$ crop incorporated 35% less C (84 g) into total edible biomass compared to the LoNH$_4^+$ crop (128 g). For N, the relative shoot content of the HiNH$_4^+$ crop (3.4%) was lower than that of the LoNH$_4^+$ crop (3.9%). In sum, the HiNH$_4^+$ crop incorporated 48% less N (7 g) into total edible biomass compared to the LoNH$_4^+$ crop (13 g).

## 4 Discussion

During long duration human space missions, bioregenerative life support systems may provide food, regenerated water, and O$_2$ for the astronauts. Given the limited availability of nutrient resources for plant production in this scenario, recycling and reuse of nutrients such as N from human urine is important. Depending on the upstream mineralization process of urine, the nutrient solution may have various NH$_4^+$:NO$_3^-$ ratios and elevated NaCl concentrations. To maximize production of food, O$_2$ and clean water, crop cultivation conditions should be optimized. However, as a BLSS consists of multiple processes, the performance of the regenerative loop including ammonification and nitrification needs to be evaluated and optimized as a whole. This illustrates a possible trade-off between the overall BLSS efficiency and crop cultivation and yield, which should be

considered in a long-term perspective with continuous operation. Increased knowledge on plant responses to various optimal and sub-optimal cultivation conditions and nutrient solutions will contribute to improved computer models, BLSS efficiency and improvement in design and control of integrated processes linking waste management and crop cultivation.

## 4.1 Biomass production and morphology

In this research campaign, considerable differences were identified between lettuce plants cultivated in nutrient solutions containing high and low NH$_4^+$:N ratios. In a BLSS perspective, the results demonstrate that both NH$_4^+$:N ratios, representing considerably different scenarios of upstream waste treatment, allow plant growth and development, and thus fixation of C and N into edible biomass. There is, however, a clear impact on biomass productivity (produced amount per time) and therefore on the total production over a given time. Under the conditions tested during the 28-day crop tests performed in this campaign, the HiNH$_4^+$ crop provided 40% lower edible biomass (shoot dry weight), resulting in the incorporation of 35% less C and 48% less N into edible biomass compared to the crop cultivated at low NH$_4^+$:N. These results are in line with previous research on lettuce, illustrating that increased ammonium concentrations strongly affect growth, resulting in decreased root and shoot biomass accumulation (Qiu et al., 2014; Wenceslau et al., 2021; Du et al., 2022; Hameed et al., 2022). Furthermore, the results are in line with general effects of ammonium toxicity on plant growth, demonstrating a biomass-reducing effect of high ammonium concentrations attributed to for example oxidative stress, nutrient imbalances and reduced photosynthesis (Barickman and Kopsell, 2016; Song et al., 2021; Weil et al., 2021). In line with the biomass results, the total leaf area per plant at time of harvest was reduced by a 2-factor for the HiNH$_4^+$ plants compared to the LoNH$_4^+$ plants. This effect is supported by other reports on hydroponically grown lettuce and other plants, demonstrating lower leaf areas with increasing ammonium concentrations (Guo et al., 2007a; Guo et al., 2007b; Urlic et al., 2017; Wenceslau et al., 2021). Beyond the NH$_4^+$:N ratio, other potential stress factors include the nutrient solution's total ionic strength and the presence of Na$^+$ and Cl$^-$ added to mimic a urine recycling scenario. While several studies indicate no or minor growth retardation of lettuce cultivated in the presence of seawater, elevated electrical conductivity and/or Na$^+$ and Cl$^-$ concentrations similar to the cultivation conditions used in the presented work (Atzori et al., 2019 and references within), one should not rule out combined effects of salinity and NH$_4^+$:N ratio especially in a foreseen future closed-loop scenario with accumulating Na$^+$ and Cl$^-$ concentrations and increasing total electrical conductivity.

Calculation of PLAI throughout the crop tests offered a method to evaluate plant growth and PLAI-based growth rate without opening the closed cultivation chamber. While noticeable differences in PLAI (and thus biomass) between the HiNH$_4^+$ and LoNH$_4^+$ crops could not easily be observed until after approximately 10 days of cultivation, calculation of $\mu_{PLAI}$ indicated a difference in specific growth rate between the two
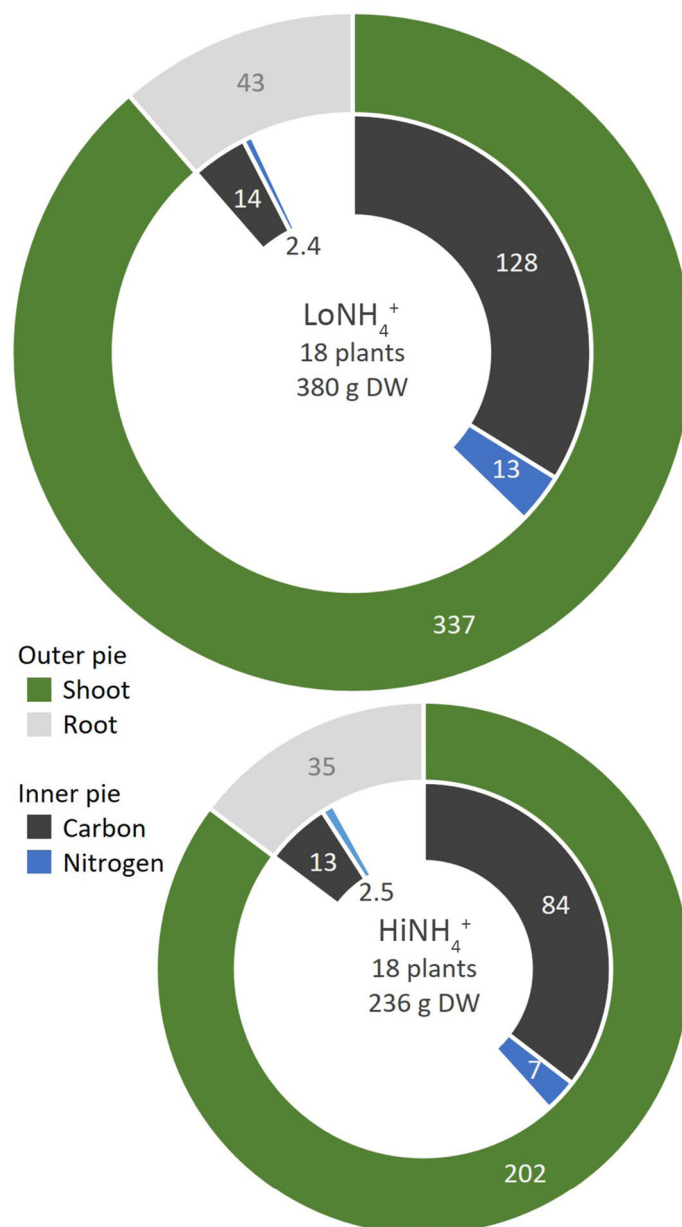
**FIGURE 7**
Incorporation of C (black) and N (blue) into shoots (green) and roots (gray) of the LoNH$_4^+$ (upper) and HiNH$_4^+$ (lower) crops. All numbers represent element or biomass dry weight in gram and relate to the full crop consisting of 18 plants. The relative difference in total pie area corresponds to the relative difference in total dry weight of the two crops.

crops starting already in the early cultivation phase. This indicates that under the conditions tested, the elevated NH$_4^+$:N ratio introduced negative effects on plant growth also during the close-to-exponential cultivation period. At the same time, this indicates that the observed NO$_2^-$ in the nutrient solution was not the main cause of the observed differences in biomass production (and thus O$_2$ production, see below). While elevated NO$_2^-$ concentrations in the nutrient solution may cause reduced growth (Hoque et al., 2008), NO$_2^-$ was not observed until the late cultivation phase of the HiNH$_4^+$ crop, at a time which μ$_{PLAI}$ of both crops had started to decrease and coincided. Coinciding μ$_{PLAI}$ towards the end of the cultivation period may be explained by reduced specific growth

rates as plants mature, and the fact that the presented growth rates are based on PLAI which, by definition, cannot exceed a factor of 1 due to a limited cultivation area and overlapping leaves.

Beyond the overall reduction in biomass production of the HiNH$_4^+$ crop, these plants displayed a significantly higher root:shoot ratio than the LoNH$_4^+$ plants, indicating a higher relative use of energy towards root growth. This is in line with previous research showing increasing root:shoot ratio with increasing NH$_4^+$:NO$_3^-$ ratio in several species, including lettuce (Zhu et al., 2020), tobacco (Walch-Liu et al., 2000) and cucumber (Zhou et al., 2017). More specifically, alteration of biomass partitioning between root and shoot is a known plant response to nutritional stress (Maskova and Herben, 2018) and NH$_4^+$:K$^+$

imbalance has been demonstrated to negatively influence carbohydrate accumulation, disturbing the root-to-shoot biomass partitioning (Zhao et al., 2020). In our study, $NH_4^+$ and $K^+$ were among the nutrient ions that demonstrated the greatest differences between the biomass content of the $HiNH_4^+$ and $LoNH_4^+$ crops. Additionally, the two crops demonstrated differences in root size and morphology. The $HiNH_4^+$ plants exhibited shorter primary and secondary roots, along with a significantly lower number of forks and links illustrating less branching. This is likely to be caused by the nutrient availability (especially of $NH_4^+$ and $NO_3^-$) and plant nutritional status, which are known to strongly influence the development of the root system (Lima et al., 2010). $NH_4^+$ is known to affect root architecture by inhibition of primary root growth and elongation, while promoting lateral branching (Liu and Von Wiren, 2017; Liu et al., 2013). Conversely, $NO_3^-$ has been shown to stimulate lateral root elongation (Lima et al., 2010; Marschner and Marschner, 2012). These observations represent valuable details for mathematical modelling of plant growth and development, as the root's surface area is critical for mass and energy transfer.

## 4.2 $O_2$ production

In total, the $HiNH_4^+$ crop produced 41% less $O_2$ than the $LoNH_4^+$. However, as the growth of the $HiNH_4^+$ plants was impaired, the $O_2$ production should be evaluated also in terms of specific production. When $O_2$ production was normalized by shoot dry weight at harvest, the amount of $O_2$ produced was 37 $mol \cdot kg^{-1}$ for both the $LoNH_4^+$ and the $HiNH_4^+$ crops. On a high level, $O_2$ production following biomass production is in line with the general mechanism of photosynthesis, converting light energy to chemical energy utilized for the synthesis and accumulation of organic matter (Evert and Eichhorn, 2013; Taiz, 2015), and hence, the photosynthetic rate is determining for biomass productivity. Furthermore, measurements of chlorophyll fluorescence on dark-adapted leaves demonstrated that the $F_v/F_m$ of both crops (0.83) was within a range indicating a healthy and well-functioning photosystem II (0.79 – 0.84) (Bjorkman and Demmig, 1987).

The total $O_2$ production, when normalized per unit leaf area at harvest, was 1.8 and 2.1 $mol \cdot m^{-2}$ for the $LoNH_4^+$ and $HiNH_4^+$ crops, respectively. Similarly, $O_2$ production per PLA demonstrates no reduction in specific $O_2$ production of the $HiNH_4^+$ plants compared to the $LoNH_4^+$ plants. On the contrary, detailed examination of the data indicates a marginal increase of the specific $O_2$ production per PLA by the $HiNH_4^+$ plants during the second and third week of the cultivation period. This indication is in line with a higher SPAD index of the leaves of the $HiNH_4^+$ plants, and a color index more towards green compared to the $LoNH_4^+$ plants. These findings are again in line with other investigations on both lettuce and species such as Arabidopsis and kohlrabi, demonstrating a higher chlorophyll concentration in leaves of plants cultivated with a higher proportion of $NH_4^+$ in the fertilizer (Blanke et al., 1996; Qiu et al., 2014; Hu et al., 2015). However, the scientific literature on chlorophyll content as a response to $NH_4^+$ concentration and $NH_4^+:NO_3^-$ ratio demonstrate complex relationships and varying results. Song et al. (2021) demonstrated that lettuce and cabbage chlorophyll content was

higher in plants exposed to an $NH_4^+:NO_3^-$ ratio of 50:50, than both 0:100 and 100:0, while Zhu et al. (2020) reported a higher chlorophyll concentration in lettuce seedlings exposed to an $NH_4^+:NO_3^-$ ratio 25:75 than both 100:0, 50:50 and 0:100. Studies of other species also show varying results, for example, an increase in chlorophyll content with increasing $NH_4^+:NO_3^-$ ratios was not discovered in kale (Assimakopoulou et al., 2019). Different theories are proposed to explain an increased chlorophyll content as a response to high ammonium. The higher chlorophyll concentration may be caused by ammonium-stress inhibiting leaf expansion, resulting in a denser chlorophyll content rather than an actual total increase (Sanchez-Zabala et al., 2015). Furthermore, carbon skeletons in the leaves favor $NH_4^+$ assimilation. Based on this, it has been proposed that a higher chlorophyll content might be a strategy to increase photosynthetic $CO_2$ assimilation to produce more carbon skeletons and thereby mitigate $NH_4^+$ accumulation (Sanchez-Zabala et al., 2015).

## 4.3 Biomass composition

The 3-fold increase of root $NH_4^+$ content of the $HiNH_4^+$ plants compared to the $LoNH_4^+$ plants is comparable to the difference between the two nutrient solutions, with 3 to 5-fold elevated $NH_4^+$ concentration (at start and end, respectively) and 3 to 7-fold elevated $NH_4^+:N$ ratio in the $HiNH_4^+$ nutrient solution compared to the $LoNH_4^+$ nutrient solution. Such elevated root $NH_4^+$ content is consistent with the roots being the primary site for initial $NH_4^+$ accumulation, where it is incorporated into organic complexes, while N is typically transported to the shoots in other forms such as amino acids (Mengel and Kirkby, 2001; Marschner and Marschner, 2012). Additionally, the biomass $NO_3^-$ content varied considerably between the crops, and in line with the nutrient solution composition. The shoots and roots of the $HiNH_4^+$ plants demonstrated an 87% and 85% reduction compared to those of the $LoNH_4^+$ plants, respectively, in line with the 42% lower $NO_3^-$ concentration in the nutrient solution. A similar reduction of leaf $NO_3^-$ content with increasing $NH_4^+:N$ ratio in the nutrient solution was reported for example for rocket salad (Kim et al., 2006). The average nitrate content of the $LoNH_4^+$ and $HiNH_4^+$ edible biomass (shoots) was 6.0 and 0.8 g $NO_3$-N per kg dry weight, respectively (Table 4). Considering the shoot dry weight content (Table 2), this corresponds to 1.8 g and 0.3 g $NO_3^-$ per kg fresh weight, respectively, both below the maximum nitrate levels set by the European Union (Commission Regulation No 1258/2011).

Analyses of the shoot and root content of nutrient ions beyond N species demonstrated an overall trend of similar or lower content of both anions and cations in the $HiNH_4^+$ plants compared to the $LoNH_4^+$ plants. As demonstrated by the ionic concentration trend of the nutrient solution, all macronutrients beyond $NH_4^+$ were available at relatively stable concentrations throughout the crop tests, indicating that the differences between the two crops were not governed by nutrient availability, but rather by direct or indirect consequences of the difference in $NH_4^+$ concentration and/or $NH_4^+:N$ ratio. This is in line with reports on reduced uptake of ions such as $K^+$, $Ca^{2+}$ and $Mg^{2+}$ with increasing $NH_4^+$ concentration and $NH_4^+:NO_3^-$ ratio in the nutrient solution (Britto and Kronzucker,

2002; Savvas et al., 2006; Roosta and Schjoerring, 2008; Fallovo et al., 2009). For example, Weil et al. (2021) reported that the concentration of both $K^+$ and $Ca^{2+}$ in lettuce shoots declined significantly with increasing nutrient solution $NH_4^+$:N ratio, concluding that the uptake of cationic nutrients and the plant growth were reduced when the $NH_4^+$:N ratio exceeded 0.50 mol·mol$^{-1}$. The observed effects on nutrient ion content have been explained by antagonism (Lasa et al., 2001; Marschner and Marschner, 2012); that the $NH_4^+$ ion resembles the $K^+$ ion in radius and hydration shell size and may therefore move through $K^+$ channels (Marschner and Marschner, 2012), and that uptake of $NO_3^-$ occurs simultaneously with the uptake of $Ca^{2+}$ or $K^+$ so that an increasing proportion of $NO_3^-$ will increase the content of $Ca^{2+}$ and $K^+$ in leaves (Du et al., 2022).

The content of NaCl in the nutrient solutions, which was designed to mimic a urine recycling scenario, may have impacted plant nutrient uptake in both the high and low $NH_4^+$- scenarios. In general, excess $Na^+$ uptake lowers the uptake of essential ions and disturbs the root-shoot transport. It has been widely observed that $Na^+$, even at low levels, inhibits the transport systems for $K^+$ uptake due to the chemical similarities between the two ions (Amini and Ehsanpour, 2005; Kronzucker et al., 2013). For some functions, $Na^+$ may also replace potassium, such as for example for maintenance of vacuole osmotic potential (Wakeel et al., 2011). $Na^+$ may cause osmotic stress, which decreases the passive uptake of calcium, resulting in a lower concentration of calcium in the plant. Another possible effect of NaCl in plant nutrition, is that $Cl^-$ may antagonize the uptake of nitrate, while it assists uptake of ammonium (Song et al., 2021).

The HiNH$_4^+$ lettuce crop demonstrated a higher carbon content in both leaves and roots compared to the LoNH$_4^+$ plants. During stress conditions that affect plant growth but still allow for photosynthesis, accumulation of sugars is commonly observed Peshev and Van Den Ende, 2013). Exposed to high $NH_4^+$ concentrations, plants have been shown to synthesize sugars to provide carbon skeletons to increase $NH_4^+$ assimilation (Raab and Terry, 1994). Additionally, plants exposed to abiotic stress often accumulate reactive oxygen species (ROS). Accumulation of soluble sugars can mitigate this toxic effect caused by plant stress by contributing to ROS scavenging (Keunen et al., 2013; Peshev and Van Den Ende, 2013). Sugars can also protect chloroplasts and thereby stabilize photosynthesis under stress conditions, and they may serve as osmoprotectants ( Peshev and Van Den Ende, 2013). Additionally, the uptake of $NO_3^-$ against the electrochemical gradient requires more use of fixed carbon compared to acquisition of $NH_4^+$ (Britto and Kronzucker, 2013).

## 4.4 Nutrient consumption and nutrient solution evolution in a long-term perspective

Maximizing resource utilization limits the possibilities of flushing the hydroponic loop and restarting the system with a fresh and balanced nutrient solution. Thus, long term development of the nutrient solution needs to be understood, modelled, and ultimately

designed and controlled in a trade off with the productivity of the plants and the design and performance of upstream processes. In light of the observed effects of the $NH_4^+$:N ratio, the development of this ratio over time should be considered. The results obtained under the conditions tested indicate a preference for $NH_4^+$ during the HiNH$_4^+$ crop test, in which N consumption apparently almost exclusively could be attributed to $NH_4^+$ consumption, although one cannot rule out that a modest nitrification activity could convert some $NH_4^+$ to $NO_3^-$ and thus mask some $NO_3^-$ consumption by the plants. Also, during the LoNH$_4^+$ crop test, the consumption of $NH_4^+$ relative to total N in the system was higher than the concentration of $NH_4^+$ relative to total N in the nutrient solution. In consequence, the nutrient solution $NH_4^+$:N ratio decreased over time during both crop tests (from 0.12 to 0.02 mol·mol$^{-1}$ in the LoNH$_4^+$ crop test; from 0.49 to 0.20 in the HiNH$_4^+$ crop test). Even after a hypothetical addition of nutrient stock solutions to restore the total N concentration before an additional plant cultivation period, the initial $NH_4^+$:N ratio of the second period will be lower than that of the first (0.03 mol·mol$^{-1}$ after topping up the remaining LoNH$_4^+$ nutrient solution to the initial 11 mM total N; 0.29 mol·mol$^{-1}$ after topping up the remaining HiNH$_4^+$ nutrient solution to the initial 11 mM total N). These considerations illustrate a potential to combine high-$NH_4^+$:N stock solutions generated by upstream waste treatment processes with efficient long-term plant biomass and $O_2$ productivity despite initially reduced productivity. In a modelling perspective, it illustrates the importance of understanding the relative $NH_4^+$:$NO_3^-$ consumption in the higher plant compartment combined with the effects of the $NH_4^+$:$NO_3^-$ ratio of the mineralized waste from upstream compartments. High $NH_4^+$ to $NO_3^-$ preference has been observed in several other studies, including a study of N absorption by tomato, in which 50% of plant N was absorbed as $NH_4^+$ even though this ion represented only 10% of available N (the remaining 90% being $NO_3^-$) (Glass et al., 2002). N preference may be linked to energy considerations as uptake of $NO_3^-$ requires energy while $NH_4^+$ can be directly absorbed, hence many plants prefer to take up $NH_4^+$ if both are available (Mengel and Kirkby, 2001; Marschner and Marschner, 2012; Du et al., 2022). Additionally, $NO_3^-$ uptake is inhibited by ammonium, and lettuce appears to absorb ammonium faster than $NO_3^-$ when the source contains both N-forms (Savvas et al., 2006; Britto and Kronzucker, 2013). However, plant preference for $NH_4^+$ or $NO_3^-$ is known to vary across plant species, physiological phase and environmental conditions (Britto and Kronzucker, 2013), and thus observed N preference may only be valid for a given species, developmental stage, and cultivation conditions. An improved understanding of the $NH_4^+$ to $NO_3^-$ preference, for example as function of cultivation conditions, should be further pursued, as this may hold potential to reduce ammonium toxicity even at conditions of high $NH_4^+$:N ratios.

During the LoNH$_4^+$ crop test which required a considerable amount of nutrient stock solution feeding, accumulation of $Na^+$, $Ca^{2+}$ and to a certain extent $Cl^-$ was observed together with a marginal reduction of $K^+$. This illustrates imbalance between the system's feed rates and consumption rates. Nutrient ion levels in the nutrient stock solutions may be tuned relative to for example total N as far as charge balancing allows in order to achieve a balanced nutrient solution. Accumulation of $Na^+$ and $Cl^-$, however, represents a potential general challenge for the utilization of

mineralized human waste. Accumulation of $Na^+$ in the nutrient solution may to a certain extent be mitigated by increased plant $Na^+$ uptake rates with increasing $Na^+$ concentrations in the nutrient solution (Neocleous and Savvas, 2017; Breś et al., 2022). Nevertheless, the extent and the implications of long-term accumulation of non-nutrients in crop cultivation based on human waste are important aspects that would benefit from further attention in a BLSS perspective.

The ratio between consumed $NH_4^+$ and consumed $NO_3^-$ affects nutrient solution pH. $NH_4^+$ uptake causes release of protons and thereby reduced pH in the root zone, which again may impact nutrient uptake (Lasa et al., 2001; Marschner and Marschner, 2012; Weil et al., 2021). This effect was clearly demonstrated during the $HiNH_4^+$ crop test with a substantial amount of base added to maintain a constant pH. The $HiNH_4^+$ scenario, with an $NH_4^+$:N ratio of 0.5 mol·mol$^{-1}$ is based on urine ammonification and partly nitrification without addition of alkalinity (Larsen et al., 2021). In a BLSS scenario, the results presented illustrate that no or low alkalinity addition during the nitrification step results in increased alkalinity requirement during the crop cultivation step instead. In this case, addition of $OH^-$ during crop cultivation should be carefully balanced with appropriate anions to avoid nutrient imbalance over time. In this context, it is interesting to notice that addition of macronutrient ions prone to be present at low concentrations in mineralized urine due to precipitation (such as $Ca^{2+}$) could possibly serve a dual purpose of being a counter ion for $OH^-$ charge balancing and being a required nutrient solution supplement. Such feeding strategies must, however, be carefully tuned and consider factors such as salt availability and solubility.

## 4.5 Strategies to maximize food and $O_2$ production in a BLSS perspective

In a Lunar greenhouse perspective, cultivation area will be limited and should be utilized in an efficient way. In a scenario of constant plant density throughout the cultivation period, plants should be cultivated to an adult stage, as the plant growth rate (g per day) and the $O_2$ production rate (mol per day) are highest during the end of the cultivation period, thus increasing also the average growth rate and the average $O_2$ production rate as evaluated over the full cultivation period. However, such a strategy comes at the cost of a low utilization rate of the available cultivation area (low PLAI), especially during the first part of the cultivation period. In a more optimized scenario, initial plant density can be high to achieve a high PLAI even with small plants. As the plants grow, the plant density can be reduced to give room for the expanding plants. In such an optimized scenario, specific production per time and PLA should be considered when aiming at optimizing food (biomass) and $O_2$ production. Under the conditions tested, the specific $O_2$ production per time and PLA reached a maximum around 13 DAT (Figure 6B), indicating that adolescent lettuce plants were more effective in $O_2$ production per time and PLA than seedlings and adult plants. With $O_2$ production linked to biomass production, this period with the highest specific $O_2$ production per time and PLA coincides with the period of highest specific growth rate (here estimated as $\mu_{PLAI}$;

Figure 4). Thus, in an optimized scenario with dynamic plant density to continuously operate at a high PLAI, the results obtained under the conditions tested suggest that plants should be cultivated up to approximately 16 - 20 days after transplant (26 - 30 days after germination) to maintain a maximized specific biomass (food) production per time and PLA and a maximized specific $O_2$ production per time and PLA. Furthermore, it is interesting to notice the indication of a higher $O_2$ production per time and PLA of the $HiNH_4^+$ crop compared to that of the $LoNH_4^+$ crop (Figure 6B), illustrating that as long as PLAI is kept high, $O_2$ productivity may be high even under cultivation conditions suboptimal for growth. Such an effect, that may be attributed to the plant's complex physiological response to mitigate suboptimal cultivation conditions, is especially interesting considering the possible need to accept suboptimal conditions for a given BLSS step in order to maximize the total efficiency of the whole loop.

## 5 Conclusion

The results of this study demonstrate the importance of understanding and considering direct and indirect effects of upstream waste processing on crop cultivation in BLSS. The urine utilization scenarios of 0.1 and 0.5 mol·mol$^{-1}$ $NH_4^+$:N demonstrated significant effects on plant development, plant nutrient composition and $O_2$ production. Under the conditions tested, plants cultivated at the high $NH_4^+$:N ratio demonstrated a high preference for ammonium combined with a reduced specific growth rate and thus a reduced total biomass production. $O_2$ production per time and projected leaf area reached a maximum during the adolescent plant phase, coinciding with exponential growth and indicating a strong relationship between biomass and $O_2$ production. Interestingly, the specific $O_2$ production per time and projected leaf area was marginally higher for the plants cultivated at high $NH_4^+$:N ratio, in line with a higher chlorophyll content. In a life support perspective, the results illustrate design concepts for crop cultivation strategies depending on the performance of upstream processes (e.g. urine mineralization and high/low $NH_4^+$:N) and downstream needs (food or $O_2$). In addition, parameters such as plant density and cultivation duration may be adjusted or balanced against each other to optimize performance. Ultimately, the results may guide the design and control of both crop cultivation and other processes in a regenerative BLSS loop towards a common trade-off and to achieve a greater good rather than optimizing individual processes.

The unique features of the ESA MELiSSA Plant Cultivation Unit (PCU) with its gas-tight atmospheric and hydroponic loops with extensive monitoring and control enabled collection of comprehensive and detailed data on crop $O_2$ production, plant growth via image-based analyses, and nutrient solution dynamics throughout the entire cultivation period. Together with future expanded capabilities of the PCU, such as analyses of $CO_2$ consumption and water production, this will contribute to improved understanding of plant responses and further advancement of computer models for predictions of plant growth and production in various BLSS and cultivation scenarios.

This study represents a further advancement towards increased waste- and resource recycling in plant-based food production systems. A deeper understanding of these processes and their impacts is crucial for the production of food and for the regeneration of water and $O_2$ in future human space exploration. Additionally, considering relevant terrestrial challenges such as depletion of mineral resources and pollution of ground waters due to nutrient runoff, nutrient recycling fuels sustainable agriculture also on Earth. Exploitation of waste streams for plant production illustrates synergies between space exploration and terrestrial food production, and knowledge on plant responses to different resource utilization scenarios improves the development and design of systems and processes for both Earth and space.

## Data availability statement

The raw data supporting the conclusions of this article will be made available by the authors, without undue reservation.

## Author contributions

ØJ, MS and A-IJ designed the experiment. MS, ØJ, AP and CQ executed the crop tests and performed analyses and calculations. All authors contributed to interpretation of results. MS and ØJ prepared the draft manuscript. All authors contributed to the article and submitted and approved the submitted section.

## Funding

## Acknowledgments

## Conflict of interest

CQ is employed by EnginSoft S.p.a.

The remaining authors declare that the research was conducted in the absence of any commercial or financial relationships that could be construed as a potential conflict of interest.

## Publisher's note

All claims expressed in this article are solely those of the authors and do not necessarily represent those of their affiliated organizations, or those of the publisher, the editors and the reviewers. Any product that may be evaluated in this article, or claim that may be made by its manufacturer, is not guaranteed or endorsed by the publisher.

## References

Acosta-Motos, J. R., Ortuno, M. F., Bernal-Vicente, A., Diaz-Vivancos, P., Sanchez-Blanco, M. J., and Hernandez, J. A. (2017). Plant responses to salt stress: adaptive mechanisms. *Agronomy-Basel* 7. doi: 10.3390/agronomy7010018

Amini, F., and Ehsanpour, A. A. (2005). Soluble Proteins, Proline, Carbohydrates and Na +/K+ Changes in Two Tomato (Lycopersicon esculentum Mill.) Cultivars under in *vitro* Salt Stress. *Am. J. Biochem. Biotechnol.* 1, 212–216. doi: 10.3844/ajbbsp.2005.212.216

Andrews, M., Raven, J. A., and Lea, P. J. (2013). Do plants need nitrate? The mechanisms by which nitrogen form affects plants. *Ann. Appl. Biol.* 163, 174–199. doi: 10.1111/aab.12045

Assimakopoulou, A., Salmas, I., Kounavis, N., Bastas, A. I., Michopoulou, V., and Michail, E. (2019). The impact of ammonium to nitrate ratio on the growth and nutritional status of kale. *Notulae Botanicae Horti Agrobotanici Cluj-Napoca* 47, 848–859. doi: 10.15835/nbha47311466

Atzori, G., Mancuso, S., and Masi, E. (2019). Seawater potential use in soilless culture: A review. *Scientia Hortic.* 249, 199–207. doi: 10.1016/j.scienta.2019.01.035

Barickman, T. C., and Kopsell, D. A. (2016). Nitrogen form and ratio impact Swiss chard (Beta vulgaris subsp cicla) shoot tissue carotenoid and chlorophyll concentrations. *Scientia Hortic.* 204, 99–105. doi: 10.1016/j.scienta.2016.04.007

Berkovich, Y. A., Chetirkin, P. V., Wheeler, R. M., and Sager, J. C. (2004). Evaluating and optimizing horticultural regimes in space plant growth facilities. *Adv. Space Res.* 34, 1612–1618. doi: 10.1016/j.asr.2003.08.080

Bjorkman, O., and Demmig, B. (1987). Photon Yield of O-2 Evolution and Chlorophyll Fluorescence Characteristics at 77-K among Vascular Plants of Diverse Origins. *Planta* 170, 489–504. doi: 10.1007/BF00402983

Blanke, M. M., Bacher, W., Pring, R. J., and Baker, E. A. (1996). Ammonium nutrition enhances chlorophyll and glaucousness in Kohlrabi. *Annals of Botany* 78, 599–604.

Bonvin, C., Etter, B., Udert, K. M., Frossard, E., Nanzer, S., Tamburini, F., et al. (2015). Plant uptake of phosphorus and nitrogen recycled from synthetic source-separated urine. *Ambio* 44 Suppl 2, S217–S227. doi: 10.1007/s13280-014-0616-6

Breś, W., Kleiber, T., Markiewicz, B., Mieloszyk, E., and Mieloch, M. (2022). The effect of naCl stress on the response of lettuce (Lactuca sativa L.). *Agronomy* 12, 244. doi: 10.3390/agronomy12020244

Britto, D. T., and Kronzucker, H. J. (2002). NH4+ toxicity in higher plants: a critical review. *J. Plant Physiol.* 159, 567–584. doi: 10.1078/0176-1617-0774

Britto, D. T., and Kronzucker, H. J. (2013). Ecological significance and complexity of N-source preference in plants. *Ann. Bot.* 112, 957–963. doi: 10.1093/aob/mct157

Chinnusamy, V., Zhu, J., and Zhu, J. K. (2006). Salt Stress Signaling and Mechanisms of Plant Salt Tolerance. In: Setlow, J.K. (eds) *Genetic Engineering.* Genetic Engineering: Principles and Methods (Boston, MA: Springer). 27, 141–177. doi: 10.1007/0-387-25856-6_9

De Bang, T. C., Husted, S., Laursen, K. H., Persson, D. P., and Schjoerring, J. K. (2021). The molecular-physiological functions of mineral macronutrients and their

consequences for deficiency symptoms in plants. *New Phytol.* 229, 2446–2469. doi: 10.1111/nph.17074

Du, K. K., Zhang, J. L., Han, Y. Y., Hao, J. H., Qin, X. X., Liu, C. J., et al. (2022). Effects of varying NO3-:NH4+ Ratios on lettuce (Lactuca sativa L.) nitrogen metabolism. *Pakistan J. Bot.* 54, 2081–2088. doi: 10.30848/PJB2022-6(37)

Evert, R. F., and Eichhorn, S. E. (2013). *Raven biology of plants* (Peter Marshall, Macmillan Education).

Fallovo, C., Colla, G., Schreiner, M., Krumbein, A., and Schwarz, D. (2009). Effect of nitrogen form and radiation on growth and mineral concentration of two Brassica species. *Scientia Hortic.* 123, 170–177. doi: 10.1016/j.scienta.2009.09.003

Glass, A. D. M., Britto, D. T., Kaiser, B. N., Kinghorn, J. R., Kronzucker, H. J., Kumar, A., et al. (2002). The regulation of nitrate and ammonium transport systems in plants. *J. Exp. Bot.* 53, 855–864. doi: 10.1093/jexbot/53.370.855

Godia, F., Albiol, J., Montesinos, J. L., Perez, J., Creus, N., Cabello, F., et al. (2002). MELISSA: a loop of interconnected bioreactors to develop life support in space. *J. Biotechnol.* 99, 319–330. doi: 10.1016/S0168-1656(02)00222-5

Guo, S. W., Chen, G., Zhou, Y., and Shen, Q. R. (2007b). Ammonium nutrition increases photosynthesis rate under water stress at early development stage of rice (Oryza sativa L.). *Plant Soil* 296, 115–124. doi: 10.1007/s11104-007-9302-9

Guo, S. W., ZHOU, Y., GAO, Y. X., LI, Y., and SHEN, Q. R. (2007c). New insights into the nitrogen form effect on photosynthesis and photorespiration. *Pedosphere* 17, 601–610. doi: 10.1016/S1002-0160(07)60071-X

Guo, S., Zhou, Y., Shen, Q., and Zhang, F. (2007a). Effect of ammonium and nitrate nutrition on some physiological processes in higher plants - Growth, photosynthesis, photorespiration, and water relations. *Plant Biol.* 9, 21–29. doi: 10.1055/s-2006-924541

Halbert-Howard, A., Häfner, F., Karlowsky, S., Schwarz, D., and Krause, A. (2021). Evaluating recycling fertilizers for tomato cultivation in hydroponics, and their impact on greenhouse gas emissions. *Environ. Sci. pollut. Res.* 28, 59284–59303. doi: 10.1007/s11356-020-10461-4

Hameed, M. K., Umar, W., Razzaq, A., Aziz, T., Maqsood, M. A., Wei, S. W., et al. (2022). Differential metabolic responses of lettuce grown in soil, substrate and hydroponic cultivation systems under NH4+/NO3- application. *Metabolites* 12. doi: 10.3390/metabo12050444

Hoque, M. M., Ajwa, H. A., and Smith, R. (2008). Nitrite and ammonium toxicity on lettuce grown under hydroponics. *Commun. Soil Sci. Plant Anal.* 39, 207–216. doi: 10.1080/00103620701759194

Hu, L. L., Yu, J. H., Liao, W. B., Zhang, G. B., Xie, J. M., Lv, J., et al. (2015). Moderate ammonium:nitrate alleviates low light intensity stress in mini Chinese cabbage seedling by regulating root architecture and photosynthesis. *Scientia Horticulturae* 186, 143–153.

Keunen, E., Peshev, D., Vangronsveld, J., Van Den Ende, W., and Cuypers, A. (2013). Plant sugars are crucial players in the oxidative challenge during abiotic stress: extending the traditional concept. *Plant Cell Environ.* 36, 1242–1255. doi: 10.1111/pce.12061

Khodadad, C. L. M., Hummerick, M. E., Spencer, L. E., Dixit, A. R., Richards, J. T., Romeyn, M. W., et al. (2020). Microbiological and nutritional analysis of lettuce crops grown on the international space station. *Front. Plant Sci.* 11. doi: 10.3389/fpls.2020.00199

Kim, S. J., Kawaharada, C., and Ishii, G. (2006). Effect of ammonium: nitrate nutrient ratio on nitrate and glucosinolate contents of hydroponically-grown rocket salad (Eruca sativa Mill.). *Soil Sci. Plant Nutr.* 52, 387–393. doi: 10.1111/j.1747-0765.2006.00048.x

Kronzucker, H. J., Coskun, D., Schulze, L. M., Wong, J. R., and Britto, D. T. (2013). Sodium as nutrient and toxicant. *Plant Soil* 369, 1–23. doi: 10.1007/s11104-013-1801-2

Larsen, T. A., Riechmann, M. E., and Udert, K. M. (2021). State of the art of urine treatment technologies: A critical review. *Water Research X*, 13. doi: 10.1016/j.wroa.2021.100114

Lasa, B., Frechilla, S., Lamsfus, C., and Aparicio-Tejo, P. M. (2001). The sensitivity to ammonium nutrition is related to nitrogen accumulation. *Scientia Hortic.* 91, 143–152. doi: 10.1016/S0304-4238(01)00239-4

Lima, J. E., Kojima, S., Takahashi, H., and Von Wiren, N. (2010). Ammonium triggers lateral root branching in Arabidopsis in an AMMONIUM TRANSPORTER1;3-dependent manner. *Plant Cell* 22, 3621–3633. doi: 10.1105/tpc.110.076216

Liu, Y., Lai, N. W., Gao, K., Chen, F. J., Yuan, L. X., and Mi, G. H. (2013). Ammonium inhibits primary root growth by reducing the length of meristem and elongation zone and decreasing elemental expansion rate in the root apex in arabidopsis thaliana. *PloS One* 8. doi: 10.1371/journal.pone.0061031

Liu, Y., and Von Wiren, N. (2017). Ammonium as a signal for physiological and morphological responses in plants. *J. Exp. Bot.* 68, 2581–2592. doi: 10.1093/jxb/erx086

Marschner, H., and Marschner, P. (2012). *Marschner's mineral nutrition of higher plants* (London, UK: Elsevier).

Maskova, T., and Herben, T. (2018). Root:shoot ratio in developing seedlings: How seedlings change their allocation in response to seed mass and ambient nutrient supply. *Ecol. Evol.* 8, 7143–7150. doi: 10.1002/ece3.4238

Mauerer, M., Rocksch, T., Dannehl, D., Schuch, I., Mewis, I., Förster, N., et al. (2018). Impact of different concentrations of nitrified urine in a recirculating nutrient solution on growth, yield and quality of lettuce. *DGG Proc.* 8, 1–5. doi: 10.5288/dgg-pr-mm-2018

Mengel, K., and Kirkby, E. A. (2001). *Principles of plant nutrition 5th edition* (Dordrecht, Netherlands: Kluwer Academic Publishers).

Neocleous, D., and Savvas, D. (2017). Simulating NaCl accumulation in a closed hydroponic crop of zucchini: Impact on macronutrient uptake, growth, yield, and photosynthesis. *J. Plant Nutr. Soil Sci.* 180, 283–293. doi: 10.1002/jpln.201600338

Pannico, A., Cimini, G., Quadri, C., Paradiso, R., Bucchieri, L., Rouphael, Y., et al. (2022). A plant characterization unit for closed life support. *Front. Astronomy Space Sci.* 9. doi: 10.3389/fspas.2022.820752

Pannico, A., El-Nakhel, C., Kyriacou, M. C., Giordano, M., Stazi, S. R., De Pascale, S., et al. (2019). Combating micronutrient deficiency and enhancing food functional quality through selenium fortification of select lettuce genotypes grown in a closed soilless system. *Front. Plant Sci.* 10. doi: 10.3389/fpls.2019.01495

Peiro, E., Pannico, A., Colleoni, S. G., Bucchieri, L., Rouphael, Y., De Pascale, S., et al. (2020). Air distribution in a fully-closed higher plant growth chamber impacts crop performance of hydroponically-grown lettuce. *Front. Plant Sci.* 11. doi: 10.3389/fpls.2020.00537

Peshev, D., and Van Den Ende, W. (2013). "Sugars as antioxidants in plants," in *Crop improvement under adverse conditions*. Eds. N. Tuteja and S. S. Gill (London: Springer).

Qiu, Z. P., Yang, Q. C., and Liu, W. K. (2014). Effects of nitrogen fertilizer on nutritional quality and root secretion accumulation of hydroponic lettuce. *Int. Symposium New Technol. Environ. Control Energy-Saving Crop Production Greenhouse Plant Factory - Greensys 2013* 1037, 679–685. doi: 10.17660/ActaHortic.2014.1037.87

Raab, T. K., and Terry, N. (1994). Nitrogen-source regulation of growth and photosynthesis in beta-vulgaris L. *Plant Physiol.* 105, 1159–1166. doi: 10.1104/pp.105.4.1159

Roosta, H. R., and Schjoerring, J. K. (2008). Effects of nitrate and potassium on ammonium toxicity in cucumber plants. *J. Plant Nutr.* 31, 1270–1283. doi: 10.1080/01904160802135050

Rouphael, Y., Petropoulos, S. A., Cardarelli, M., and Colla, G. (2018). Salinity as eustressor for enhancing quality of vegetables. *Scientia Hortic.* 234, 361–369. doi: 10.1016/j.scienta.2018.02.048

Sanchez-Zabala, J., Gonzalez-Murua, C., and Marino, D. (2015). Mild ammonium stress increases chlorophyll content in Arabidopsis thaliana. *Plant Signaling Behav.* 10. doi: 10.4161/15592324.2014.991596

Savvas, D., Passam, H. C., Olympios, C., Nasi, E., Moustaka, E., Mantzos, N., et al. (2006). Effects of ammonium nitrogen on lettuce grown on pumice in a closed hydroponic system. *Hortscience* 41, 1667–1673. doi: 10.21273/HORTSCI.41.7.1667

Song, J., Yang, J., and Jeong, B. R. (2021). Growth, Quality, and Nitrogen Assimilation in Response to High Ammonium or Nitrate Supply in Cabbage (Brassica campestris L.) and Lettuce (Lactuca sativa L.). *Agronomy-Basel* 11. doi: 10.3390/agronomy11122556

Taiz, L. (2015). *Plant Physiology and Development, sixth edition* (Sunderland CT, USA: Sinauer Associates Inc).

Udert, K. M., Larsen, T. A., and Gujer, W. (2006). Fate of major compounds in source-separated urine. *Water Sci. Technol.* 54, 413–420. doi: 10.2166/wst.2006.921

Udert, K. M., and Wachter, M. (2012). Complete nutrient recovery from source-separated urine by nitrification and distillation. *Water Res.* 46, 453–464. doi: 10.1016/j.watres.2011.11.020

Urlic, B., Spika, M. J., Becker, C., Klaring, H. P., Krumbein, A., Ban, S. G., et al. (2017). Effect of NO3 and NH4 concentrations in nutrient solution on yield and nitrate concentration in seasonally grown leaf lettuce. *Acta Agriculturae Scandinavica Section B-Soil Plant Sci.* 67, 748–757. doi: 10.1080/09064710.2017.1347704

Wakeel, A., Farooq, M., Qadir, M., and Schubert, S. (2011). Potassium substitution by sodium in plants. *Crit. Rev. Plant Sci.* 30, 401–413. doi: 10.1080/07352689.2011.587728

Walch-Liu, P., Neumann, G., Bangerth, F., and Engels, C. (2000). Rapid effects of nitrogen form on leaf morphogenesis in tobacco. *J. Exp. Bot.* 51, 227–237. doi: 10.1093/jexbot/51.343.227

Weil, S., Barker, A. V., Zandvakili, O. R., and Etemadi, F. (2021). Plant growth and calcium and potassium accumulation in lettuce under different nitrogen regimes of ammonium and nitrate nutrition. *J. Plant Nutr.* 44, 270–281. doi: 10.1080/01904167.2020.1806313

Wenceslau, D., Oliveira, D. F., Rabelo, H., Ferbonink, G. F., Gomes, L. A. A., Leonel, E. C. A., et al. (2021). Nitrate concentration and nitrate/ammonium ratio on lettuce grown in hydroponics in Southern Amazon. *Afr. J. Agric. Res.* 17, 862–868.

Wheeler, R. M., Stutte, G. W., Subbarao, G. V., and Yorio, N. C. (2002). "Plant growth and human life support for space travel," in *Handbook of plant and crop physiology*, 2 ed. Ed. M. Pessarakli (New York: Marcel Dekker Inc).

Zhao, H. Y., Sun, S. M., Zhang, L. H., Yang, J. J., Wang, Z. Y., Ma, F. W., et al. (2020). Carbohydrate metabolism and transport in apple roots under nitrogen deficiency. *Plant Physiol. Biochem.* 155, 455–463. doi: 10.1016/j.plaphy.2020.07.037

Zheng, G., and Moskal, L. M. (2009). Retrieving leaf area index (LAI) using remote sensing: theories, methods and sensors. *Sensors* 9, 2719–2745. doi: 10.3390/s90402719

Zhou, J. Y., Wang, M., Sun, Y. M., Gu, Z. C., Wang, R. R., Saydin, A., et al. (2017). Nitrate increased cucumber tolerance to fusarium wilt by regulating fungal toxin production and distribution. *Toxins* 9. doi: 10.3390/toxins9030100

Zhu, X., Yang, R., Han, Y. Y., Hao, J. H., Liu, C. J., and Fan, S. X. (2020). Effects of different NO3-:NH4+ ratios on the photosynthesis and ultrastructure of lettuce seedlings. *Horticulture Environ. Biotechnol.* 61, 459–472. doi: 10.1007/s13580-020-00242-w